

1 **Title Page**

2 *Schistosoma mansoni* infection alters the host pre-vaccination environment resulting in blunted Hepatitis
3 B vaccination immune responses.

4
5 Roshell Muir^{*1}, Talibah Metcalf^{*1}, Slim Fourati^{*2}, Yannic Bartsch³, Jacqueline Kyosiimire Lugeswa⁴,
6 Glenda Canderan⁵, Galit Alter³, Enoch Muyanja^{2,6}, Brenda Okech⁶, Teddy Namatovu⁶, Irene Namara⁶,
7 Annemarie Namuniina⁶, Ali Ssetaala⁶, Juliet Mpendo⁶, Annet Nanvubya⁶, Paul Kato Kitandwe⁴, Bernard
8 S. Bagaya⁷, Noah Kiwanuka⁸, Jacent Nassuna⁸, Victoria Menya Biribawa⁶, Alison M. Elliott^{4,9}, Claudia J.
9 de Dood¹⁰, William Senyonga⁴, Priscilla Balungi⁴, Pontiano Kaleebu⁴, Yunia Mayanja⁴, Mathew
10 Odongo⁴, Pat Fast^{11,12}, Matt A. Price^{11,13}, Paul L.A.M. Corstjens¹⁴, Govert J. van Dam¹⁵, Anatoli
11 Kamali^{6,11}, Rafick Pierre Sekaly², Elias K Haddad¹.

12
13 ^{*}These three authors share first authorship.

14
15 ¹Division of Infectious Diseases and HIV Medicine, Department of Medicine, Drexel University College
16 of Medicine, Philadelphia, Pennsylvania, USA.

17 ²PATRU, School of Medicine, Emory University, Atlanta, GA, USA

18 ³Ragon Institute of MGH, MIT, and Harvard, Cambridge, MA, USA.

19 ⁴MRC/UVRI and LSHTM Uganda Research Unit, Entebbe, Uganda

20 ⁵Department of Medicine, Allergy and Immunology, University of Virginia, Charlottesville, VA, USA

21 ⁶UVRI-IAVI HIV Vaccine Program, Entebbe, Uganda

22 ⁷Department of Immunology and Molecular Biology, School of Biomedical Sciences, Makerere

23 University, College of Health Sciences, Kampala-Uganda

24 ⁸Department of Epidemiology and Biostatistics, School of Public Health, Makerere University, College of
25 Health Sciences, Kampala-Uganda

26 ⁹Department of Clinical Research, London School of Hygiene and Tropical Medicine, London, UK

27 ¹⁰Department of Cell and Chemical Biology, Leiden University Medical Center, Leiden, Netherlands

28 ¹¹International AIDS Vaccine Initiative, New York, NY, USA

29 ¹²Pediatric Infectious Diseases, Stanford University School of Medicine, Palo Alto, CA, USA

30 ¹³Department of Epidemiology and Biostatistics, University of California at San Francisco, San Francisco,
31 USA

32 ¹⁴Department of Cell and Chemical Biology, Leiden University Medical Center, Leiden, the Netherlands

33 ¹⁵Department of Parasitology, Leiden University Medical Center, Leiden, the Netherlands

34 ¹⁶IAVI, New York, New York, USA, and Nairobi, Kenya

35

36 Correspondence should be addressed to Elias K. Haddad, Ph.D., Division of Infectious Diseases and HIV
37 Medicine, Department of Medicine, Drexel University College of Medicine, 245 N. 15th Street, MS-461,
38 Philadelphia, Pennsylvania, 19102, USA. Telephone: E-mail: ee336@drexel.edu

39

40 **Conflicts of Interest**

41 The authors have declared that no conflict of interest exists.

42

43 **Short Title**

44 Schistosomiasis and Hepatitis B vaccination responses

45

46

47

48

49

50

51

52 **Abstract**

53 The impact of endemic infections on protective immunity is critical to inform vaccination strategies. In
54 this study, we assessed the influence of *Schistosoma mansoni* infection on host responses in a Ugandan
55 fishing cohort given a Hepatitis B (HepB) vaccine. Concentrations of schistosome-specific circulating
56 anodic antigen (CAA) pre-vaccination showed a significant bimodal distribution associated with HepB
57 titers, which were lower in individuals with high CAA. We established that participants with high CAA
58 had significantly lower frequencies of circulating T follicular helper (cTfh) subpopulations pre- and post-
59 vaccination and higher regulatory T cells (Tregs) post-vaccination. Polarization towards higher
60 frequencies of Tregs: cTfh cells can be mediated by changes in the cytokine environment favoring Treg
61 differentiation. In fact, we observed higher levels of CCL17 and soluble IL-2R pre-vaccination (important
62 for Treg recruitment and development), in individuals with high CAA that negatively associated with
63 HepB titers. Additionally, alterations in pre-vaccination monocyte function correlated with HepB titers,
64 and changes in innate-related cytokines/chemokine production were associated with increasing CAA
65 concentration. We report, that by influencing the immune landscape, schistosomiasis has the potential to
66 modulate immune responses to HepB vaccination. These findings highlight multiple *Schistosoma*-related
67 immune associations that could explain abrogated vaccine responses in communities with endemic
68 infections.

69

70 **Author Summary**

71 Schistosomiasis drives host immune responses for optimal pathogen survival, potentially altering host
72 responses to vaccine-related antigen. Chronic schistosomiasis and co-infection with hepatotropic viruses
73 are common in countries where schistosomiasis is endemic. We explored the impact of *Schistosoma*
74 *mansoni* (*S. mansoni*) infection on Hepatitis B (HepB) vaccination of individuals from a fishing
75 community in Uganda. We demonstrate that high schistosome-specific antigen (circulating anodic
76 antigen, CAA) concentration pre-vaccination, is associated with lower HepB antibody titers post-

77 vaccination. We show higher pre-vaccination levels of cellular and soluble factors in instances of high
78 CAA that are negatively associated with HepB antibody titers post-vaccination, which coincided with
79 lower frequencies of circulating T follicular helper cell populations (cTfh), proliferating antibody
80 secreting cells (ASCs), and higher frequencies of regulatory T cells (Tregs). We also show that monocyte
81 function is important in HepB vaccine responses, and that high CAA is associated with alterations in the
82 early innate cytokine/chemokine microenvironment. Our findings suggest that in individuals with high
83 CAA and likely high worm burden, schistosomiasis creates and sustains an environment that is polarized
84 against optimal host immune responses to the vaccine, which puts many endemic communities at risk for
85 infection against HepB and other diseases that are preventable by vaccines.

86

87

88

89

90

91

92

93

94

95

96

97

98

99

100

101

102 **Introduction**

103 While vaccines have reshaped public health and saved millions of lives from the threat of many
104 infectious diseases (1), inadequate immune responses to vaccination remain a challenge, with a range of
105 contributory causes, such as chronic illnesses, including those stemming from helminth worm infections
106 (2-4). Schistosomiasis is a neglected tropical disease (NTD) caused by parasitic flatworms from three
107 main *Schistosoma* spp. that often develops into a chronic infection in endemic populations, with 90% of
108 all infections found in sub-Saharan Africa. An estimated four million people in Uganda are infected
109 with *S. mansoni* and about 55% of the population is at risk of infection (5, 6). Currently, treatment with
110 Praziquantel (PZQ) is the only safe and effective protocol against infection with *Schistosoma* spp. and
111 control of Schistosomiasis in endemic regions involves periodic administration of PZQ to communities
112 (7).

113 Chronic schistosomiasis with hepatitis B virus (HBV) and hepatitis C virus (HCV) co-infection is
114 common in countries where schistosomiasis is endemic. There is also evidence that *S. mansoni* co-
115 infection with hepatotropic viruses may exacerbate resultant hepatic pathology (8). In Uganda, more than
116 1.4 million adults are chronically infected with hepatotropic viruses, and the prevalence of HBV is
117 approximately 8.5% (9, 10) with an increased incidence in the Lake Victoria fishing communities (11).
118 While vaccination against Hepatitis B (HepB) is highly effective in the prevention of infection, there are
119 still ~ 800,000 deaths attributable to acute and chronic HepB disease annually (12). Furthermore, 5-10%
120 of individuals do not mount an effective antibody response to HepB vaccination (13). There is a need for
121 improved understanding of the immunological responses during vaccination to ensure effective responses
122 in compromised host immune systems.

123 *Schistosoma* spp. induces strong host T helper 2 (Th2) responses, but also go on to induce
124 regulatory T cell (Treg) responses which in turn curbs T helper immunity (14, 15). Specifically, the
125 chronic phase develops due to continual exposure to the soluble egg antigen (SEA) of schistosome eggs

126 in the host tissues, driving immune-pathology and progressing to granuloma formation, characterized by
127 an increase in lymphocytes (CD4⁺ T cells) producing T-helper-2 (Th2) cytokines such as interleukins (IL)
128 -4, -5, and -13. This heightened Th2 response becomes suppressed over time to induce tolerance, which is
129 the major influence on worm survival in the host (16, 17). Upregulation of these responses could
130 potentially inhibit the T helper responses induced by vaccination, such as T follicular helper (Tfh)
131 responses which are critical for B cell help (18, 19), and foster conditions that cause alterations of
132 vaccine-induced antibody responses. Studies showing the effects of *Schistosoma* infection on the
133 modulation of immune responsiveness to concomitant diseases and immunization are not without
134 controversy; however, the consensus is this infection can diminish or alter immune responses to non-
135 schistosome antigens. These responses may lead to either beneficial or detrimental outcomes for the host.
136 In the case of vaccine responses, animal models of malaria (20) , bacteria (21) and HepB (22) show
137 reduced protective effects; and human vaccination studies have shown lower levels of vaccine-specific
138 antibody in *Schistosoma*-infected children (23, 24), and in HepB vaccination of adults (25, 26). However,
139 the impact of *S. mansoni* infection and worm burden on host immune response to vaccines, and to HepB
140 vaccination, is still poorly understood; and the underlying actions of immune mediators affecting these
141 responses need to be further elucidated to identify strategies to optimize vaccination effectiveness.

142 Detection of CAA (Circulating Anodic Antigen, a worm antigen regurgitated into the
143 bloodstream of the host) in serum indicates an ongoing infection, implying the presence of living
144 *Schistosoma* worms. CAA is produced at a steady level and although worm pairs do produce eggs, worms
145 do not multiply and there is a direct association of CAA serum level with worm burden. It was estimated
146 that an amount of 1-10 pg/mL blood corresponds to a single healthy worm pair (27, 28). In this study, we
147 characterized soluble and cellular immune factors at pre- and post-immunization timepoints with a HepB
148 vaccine in PZQ-treated individuals with high and low CAA and explored mechanisms which may be
149 responsible for a blunted vaccine response in individuals with high CAA and likely a high worm burden.
150 We demonstrated that *S. mansoni* infection is associated with significantly lower HepB vaccine-specific
151 antibody responses and showed these responses coincided with alterations in cytokines and chemokines

152 that are important for Tfh and Treg cell recruitment and function. We propose that a high CAA
153 concentration due to a high *S. mansoni* worm burden pre-vaccination, can reshape the baseline
154 environment, and modulate the response to vaccines.

155

156 **Results**

157 **Pre-vaccination *S. mansoni* infection negatively impacts Hepatitis B antibody titers post-vaccination**

158 Seventy-five participants for the present study were recruited in Uganda among fishing
159 communities on the northern shores of Lake Victoria, where schistosomiasis is endemic and various
160 samples were collected at multiple timepoints for subsequent study analyses (Fig 1, S1 Table). HepB
161 antibody titers (anti-HBs) were determined in the serum at D0, M7 (1 month post-2nd boost) and M12 (6
162 months post-2nd boost) to look at levels pre-vaccine, as well as short-term and longer-term post-
163 vaccination antibody responses after completion of the immunization series (Fig 1 and S1 Table). A
164 circulating anodic antigen (CAA) detection assay (29-32) was also determined pre-vaccination (D0) in the
165 serum of enrolled participants (Fig 1 and S1 Table). The presence of CAA indicates an ongoing *S.*
166 *mansoni* infection, with CAA concentration closely linked to worm burden (27, 28) and those found to be
167 infected were treated with PZQ at day 12 (D12) post-vaccination (Fig 1). The results show that CAA
168 values displayed a bimodal distribution. The cutoff separating the two modes was estimated by
169 maximum-likelihood which revealed that participants could be separated into those with a CAA
170 concentration of <36 pg/mL (low or no worm burden); and those with a CAA concentration of ≥36 pg/mL
171 (higher worm burden) (Fig 2A). Importantly, CAA values from these two groups of participants were
172 significantly associated with HepB titers measured at month 7 (M7), where low CAA was associated with
173 a high titer, and high CAA with a low titer (log₁₀ fold change (FC)= -0.43, 95% confidence interval (CI)
174 [-0.053, -0.81]; P=0.028) (Fig 2B). The same trend between HepB titers and the two CAA groups
175 was observed after adjusting for age and sex (log₁₀FC= -0.38, 95% CI [0.059, -0.81]; P=0.089).

176 In acknowledging the role *S. mansoni* infection and worm burden could play in the modulation of
177 host immunity, whether the individuals at the time of the study were uninfected or infected, and the level
178 of *S. mansoni* worm burden, is important in data interpretation. For this reason, individuals were further
179 stratified into three groups using methodology from the CAA assay that allowed detection of samples as
180 low as 3pg/mL: non-infected (no) (CAA <3 pg/mL), low CAA concentration (low) (CAA 3-100 pg/mL)
181 and high CAA concentration (high) (CAA >100 pg/mL) (S1 Table) (33). Association of these three
182 groups with vaccine responses indicated higher HepB titers in non-infected individuals, followed by those
183 with low CAA and high CAA (Fig 2C and 2D). Overall, these data show an association between CAA
184 concentration pre-vaccination and vaccine-specific responses, specifically that that a higher CAA
185 concentration and likely higher worm burden, can negatively influence post-vaccination antibody titers.

186

187 **Plasma cytokines/chemokines involved in lymphocyte migration and activation are significantly**
188 **higher in *S. mansoni* infection pre-vaccination and persist at month 12 post-vaccination**

189 To elucidate any patterns of cytokine/chemokine production between infected groups pre-
190 vaccination and post-vaccination, plasma samples from non-infected and *S. mansoni*-infected individuals
191 were analyzed using multiplex cytokine/chemokine platform of more than 65 soluble factors. We
192 identified that pre-vaccination systemic levels of CCL17 (no vs. low P=0.002, no vs. high P<0.0001),
193 CCL19 (no vs. low P=0.004, no vs. high P<0.0001, low vs. high P=0.040), CXCL9 (no vs. low P=0.012,
194 no vs. high P<0.0001, low vs. high P=0.002) (Fig 3A- 3C, S2 Table), and several other cytokines and
195 chemokines implicated in lymphocyte recruitment and activation (S1A- S1F Fig, S2 Table), were
196 significantly higher in individuals with low and high CAA compared to non-infected at D0. Of interest,
197 the levels of CCL17 (no vs. high P=0.012), CCL19 (no vs. high P=0.040) and CXCL9 (no vs. high
198 P=0.004, low vs. high P=0.031) remained significantly elevated in individuals with high CAA at M12
199 post-vaccination (Fig 3A-3C, S2 Table). Furthermore, principal component analysis (PCA) analysis
200 shows that cytokine/chemokine levels pre-vaccination, cluster separately from post-vaccination time
201 points, suggesting an association between HepB vaccination and major changes in circulating

202 cytokines/chemokines that are sustained over time (up to 6 months after the last immunization, Fig 2D).
203 The relationship between alterations in these cytokines/chemokines and the levels of HepB titers, was
204 evaluated to identify biomarkers associated with a stronger humoral response to vaccination. Pre-
205 vaccination ($t=-3.01$, $P=0.004$) and M12 post-vaccination ($t=-2.40$, $P=0.020$) levels of CCL17 showed a
206 negative correlation with HepB titers at M12 (S2A and S2B Fig, S3 Table). While levels of soluble IL-2R
207 (sIL-2R) were not different in *S. mansoni* infection compared to non-infected (S2C Fig and S2 Table),
208 sIL-2R levels pre-vaccination ($t=-2.22$, $P=0.032$) and M12 post-vaccination ($t=-2.95$, $P=0.005$) were also
209 negatively correlated with HepB titers at M12 (S2D and S2E Fig, S3 Table). These observations suggest a
210 high worm burden in *S. mansoni* infection could be associated with alterations of the host
211 cytokine/chemokine response to vaccination and implicate CCL17 and potentially sIL-2R, known to
212 attract both effector and regulatory T cells (34-38).

213
214 **Frequencies of circulating T follicular helper cell populations are significantly lower pre-**
215 **vaccination which is sustained post-vaccination in *S. mansoni* infection and coincides with higher**
216 **frequencies of regulatory T cells in individuals with high CAA concentration**

217 Cellular immunological changes influenced by the cytokine environment are key in modulating
218 effective vaccine-specific humoral responses. We assessed frequencies of circulating T follicular helper
219 (cTfh) populations (39), critically involved in providing B cell help in infection and vaccination (40-42),
220 from the PBMCs of non-infected and *S. mansoni*-infected individuals by flow cytometry (S3 Fig).
221 Frequencies of cTfh1 (low vs. high $P=0.020$) and cTfh2 cells (no vs. high $P=0.012$, low vs. high $P=0.014$)
222 pre-vaccination (Fig 4A and 4B, S4 Table), were significantly lower in individuals with high CAA; and
223 cTfh1 cells remained significantly lower at M7 (low vs. high $P=0.031$) and M12 (no vs. high $P=0.030$,
224 low vs. high $P=0.004$) post-vaccination (Fig 4A, S4 Table). While differences between non-infected and
225 *S. mansoni*-infected groups for cTfh17 cells pre-vaccination did not reach statistical significance, they
226 were significantly lower in *S. mansoni*-infected individuals at M12 post-vaccination (no vs. low $P=0.024$,
227 no vs. high $P=0.006$) (Fig 4C, S4 Table). Importantly, these alterations were specific to cTfh cells, as no

228 statistically significant changes between groups were observed at any of the time points for non-cTfh cells
229 (Fig 4D). By contrast, frequencies of CXCR5⁻ regulatory T cells (Tregs), that were similar between non-
230 infected and *S. mansoni*-infected groups pre-vaccination, were significantly higher at M7 (no vs. high
231 P=0.039) and M12 (no vs. high P=0.047) post-vaccination in individuals with high CAA (Fig 4E, S4
232 Table). These results suggest that frequencies of cTfh cells, which are important for instructing B cells to
233 produce antibodies, are significantly altered in instances of high worm burden, and the concomitant
234 increase in Tregs supports the theory that worm burden could have an impact on the interplay between
235 these two subsets.

236

237 **Antibody-secreting B cells are significantly lower in instances of high worm burden and is**
238 **associated with Hepatitis B antibody titers at month 12**

239 Cellular changes were further examined in response to *S. mansoni* infection and HepB
240 vaccination by looking at the frequencies of activated B cells (ABC) and antigen-specific antibody-
241 secreting B cells (ASC) (43) (S4 Fig). Frequencies of ABCs (no vs. high P=0.048) and IgG⁺ABCs (no vs.
242 high P=0.015) were found to be significantly higher pre-vaccination in individuals with high CAA, with
243 similar results at M7 (ABC, no vs. high P=0.039; IgG⁺ABCs, no vs. high P=0.032) and M12 (ABC, no vs.
244 high P=0.040; IgG⁺ABCs, no vs. high P=0.033) post-vaccination (S5A and S5B Fig, S5 Table), indicative
245 of a hyperactivated inflammatory B cell response (41). Of importance and in sharp contrast, lower
246 frequencies of KI67⁺ASC (no vs. high P=0.040), IgG⁺ASC (no vs. high P=0.046), and IgA⁺ASC (no vs.
247 high P=0.029) populations were observed in individuals with high CAA at M12 post-vaccination (Fig 5A-
248 5C). Furthermore, assessment of the correlation between ASCs and HepB titers showed a positive
249 correlation between IgA⁺ASCs and HepB titers at M12 ($t=2.10$, P=0.041) (S5C Fig and S6 Table). These
250 results imply that an elevated worm burden can influence humoral immunity, including isotype during
251 vaccination, particularly by modulating changes in the B cell compartment resulting in a highly non-
252 specific inflammatory B cell response, and a reduction in the vaccine-specific B cell response.

253

254 **Impact of *S. mansoni* infection on Ig isotypes**

255 B cell isotype switching changes the effector functions of antibodies and improves the
256 effectiveness of the required response to infection or vaccination. Herein, B cell function was further
257 investigated in the context of Ig class-switching by treating PBMCs from non-infected and *S. mansoni*-
258 infected individuals with the TLR9 ligand CpG-ODN 2006 and analyzing the culture supernatant for Ig
259 antibodies using a multiplex bead assay. IgG4, known to be associated with *Schistosoma* reinfection (44),
260 was found to be the only subclass with significant differences between non-infected and *S. mansoni*-
261 infected at pre-vaccination, and had the highest levels in the high worm burden group (no vs. high
262 $P=0.002$, low vs. high $P=0.003$) (Fig 6A). We observed similar trends for plasma IgE pre-vaccination (no
263 vs. high $P=0.0008$, low vs. high $P=0.0001$); in contrast to CpG-induced IgG4, higher levels were
264 sustained at M12 post-vaccination (no vs. high $P=0.001$, low vs. high $P=0.002$) (S6 Fig). Furthermore, a
265 Luminex-based serologic assay was also used to quantify pre-vaccination levels of *Schistosoma*-specific
266 antibody isotypes and subclasses in the serum of participants, and the mean fluorescence intensity (MFI) of
267 *S. mansoni*-specific IgG4 was found to be significantly associated with CAA concentration ($P=0.0008$),
268 with higher levels in individuals with high CAA compared to non-infected ($P=0.0003$) and individuals
269 with low CAA ($P=0.021$) (Fig 6B). Post-vaccination, IgA levels in the supernatant of CPG-stimulated
270 PBMCs were found to be significantly different between non-infected and *S. mansoni*-infected
271 individuals, where the lowest levels were observed in individuals with high CAA (no vs. high $P=0.031$)
272 (Fig 6C). The development of antigen-specific soluble IgA is thought to be critically important in an
273 effective immune response to vaccination (45), and these results reveal that worm burden could influence
274 the host's ability to mount a specific antibody response.

275

276 **Vaccine-Specific Memory CD4⁺ T cells positively correlate with Hepatitis B antibody titers**

277 The CD4⁺ T cell memory compartment houses both the cTfh and Treg populations, which
278 showed variations in their frequencies in instances of *Schistosoma* infection pre- and post-vaccination
279 (Fig 4). To determine the impact of *S. mansoni* infection on HepB-specific memory T cells, PBMCs from

280 non-infected and *S. mansoni*-infected individuals at M7 were treated with a Hepatitis B long envelope
281 protein (HBV LEP) peptide, and CFSE⁻ cells analyzed by flow cytometry were identified as vaccine-
282 specific. Vaccine-specific memory CD4⁺ T and CD8⁺ T cells were significantly higher after peptide
283 stimulation compared to control (DMSO), and lower frequencies of proliferating CD4⁺ T cells, but not
284 CD8⁺ T cells were observed in *S. Mansoni*-infected individuals compared to non-infected (Fig 7A and
285 7B). Interestingly, and in assessing an association with HepB titers, a positive association was observed
286 between vaccine-specific memory CD4⁺ T cells and HepB titers ($t=1.85$, $P=0.073$) (Fig 7C), with a
287 concurrent significant negative correlation between vaccine-specific memory CD8⁺ T cells and HepB
288 titers ($t=-2.36$, $P=0.025$) (Fig 7D). These results highlight how CD4⁺ and CD8⁺ memory T cells may play
289 separate and antagonistic roles in their contribution to vaccination responses during infection.

290

291 **Monocyte function is positively associated with effective Hepatitis B vaccine responses**

292 Our analysis has pointed to the importance of key cytokines/chemokines involved in innate
293 responses to infection that was detected pre-vaccination, and how they may play a crucial role in
294 modulating the immune response post-vaccination in non-infected and *S. mansoni*-infected individuals
295 with various levels of worm burden. To additionally investigate the importance of innate responses, the
296 frequencies of monocyte populations were determined by flow cytometry of PBMCs from non-infected
297 and *S. mansoni*-infected participants (S7 Fig), however no differences between CAA groups were
298 observed pre-vaccination for all three monocyte populations (S8A- S8C Fig), even though CD14⁺CD16⁻
299 classical monocytes were found to negatively associate with HepB titers significantly at M7 (coef=-0.027,
300 $P=0.017$) (S8D Fig). To further elucidate the relationship between monocyte function and HepB vaccine
301 responses, THP-1 cells (a monocyte cell line) were used to carry out an antibody-dependent cellular
302 phagocytosis (ADCP) assay, and ADCP was found to positively correlate with HepB titers at M12
303 ($P=0.0008$) (Fig 8A), HepB surface antigen (HbsAg)-specific IgG1 titers ($P=0.009$) (Fig 8B), and binding
304 of HbsAg-specific antibodies to the cytotoxic Fc gamma receptor 3A (FcγR3A) ($P=0.001$) (Fig 8C),
305 indicating the importance of monocyte function in an effective humoral immune response to the Hepatitis

306 B vaccine. As we did not observe any associations between monocyte subsets and CAA concentration,
307 suggesting that monocyte frequency is not directly affected by *S. mansoni* infection, we thought it was
308 important to further examine associations of innate immune function with CAA concentration by
309 exploring the induction of cytokine/chemokines.

310

311 **Innate immune-related cytokines/chemokines are significantly lower pre-vaccination and day 12**
312 **post-vaccination in instances of high CAA concentration after TLR7/8 stimulation**

313 Toll-like receptors (TLRs) mediate innate immune responses to pathogen-associated molecules
314 (46). To investigate the importance of monocyte function in shaping the response to Hepatitis B
315 vaccination during *S. mansoni* infection, PBMCs from non-infected and *S. mansoni*-infected individuals
316 were stimulated with a viral toll-like receptor (TLR) 7/8 agonist- imidazoquinoline compound CLO97,
317 and the supernatant analyzed by multiplex bead assay for cytokines/chemokines after 18 hours of
318 stimulation. Levels of the CXC chemokine IFN- γ -inducible protein 10 (CXCL10; IP-10), which plays a
319 crucial role in activating innate immune cells, promoting dendritic cell (DC) maturation, and inducing
320 protective T cell responses (47, 48), were significantly lower in CLO97-treated supernatant from the high
321 CAA group pre-vaccination (low vs. high P=0.031) (Fig 9A, S7 Table). Furthermore, supernatant levels
322 of CCL19 (no vs. high P=0.009), CCL26 (no vs. high P=0.014), CCL27 (no vs. high P=0.007), IL-1 β (no
323 vs. high P=0.028), and IL-10 (no vs. high P=0.008, low vs. high P=0.053) were also significantly lower in
324 the high CAA group after treatment with CLO97 D12 post-vaccination (Fig 9B-9F, S7 Table).
325 Collectively, these cytokines/chemokines play important roles in early immune responses to viral
326 infection and vaccination including modulation of inflammatory responses and adaptive cell recruitment,
327 activation, and regulation (49-53). These results indicate an association between *S. mansoni* infection and
328 worm burden in the altering of the pre-vaccination, and early post-vaccination innate cytokine
329 environment.

330

331 Discussion

332 Vaccination is an essential tool in controlling the spread of infectious diseases, but variations of
333 host immune responses to vaccines across populations (endemic infections, pre-existing infections,
334 geography, biological sex, race/ethnicity) impact the generation of protective immune responses, and thus
335 how vaccines can be designed to treat populations are at greater risk for poor clinical outcomes. These
336 variations in vaccine responses, seen in communities with endemic diseases such as schistosomiasis, have
337 recently been the topic of intense investigation (3, 4). We show that pre-vaccination worm burden
338 specifically influences levels of vaccine-specific antibody production. Individuals from a Ugandan fishing
339 community cohort were stratified into non-infected and *S. mansoni*-infected with low worm burden (low
340 CAA concentration), or high worm burden (high CAA concentration) (33). We show that the pre-
341 vaccination CAA values aligned with groups categorized by low and high worm burden displayed a
342 bimodal distribution, and that increasing CAA concentration was negatively associated with vaccine-
343 specific antibody levels. This association also served as the premise for further investigation to delineate
344 what molecules and cell populations were at play, and responsible for these changes in vaccine-related
345 immune responses post-vaccination.

346 The major strength of this study lies in this unique cohort, which allowed analysis of individuals
347 pre-vaccination and post-vaccination, with different concentrations of CAA and likely different levels of
348 worm burden from direct exposure, or no *S. mansoni* infection at all; and allowed us to comment
349 definitively on the impact of baseline *S. mansoni* infection on vaccine-induced responses, and more
350 specifically if these induced responses were affected by worm burden. Notably, CAA concentration
351 indicates an active infection and the presence of living worms, allowing for serum CAA concentration to
352 be directly associated with worm burden (27, 28). While egg count data was determined, they are
353 approximately 50% sensitive when done on a single stool sample (54). Furthermore, as the worms
354 themselves do not multiply, egg count data only indicates worm pairs producing eggs and not quantitative
355 data on overall worm burden (55). Our analysis of vaccine-specific antibody titers, cytokines/chemokines,
356 and immune and adaptive cellular responses also allowed us to identify the links between high *S. mansoni*

357 worm burden and lower HepB vaccine responses. While the outcomes of this present study were based
358 solely on the influence of *S. Mansoni* infection on HepB vaccination, we believe the results have the
359 potential to direct other immunization programs in schistosomiasis-impacted communities where repeated
360 exposure is likely.

361 Our analysis showed induction of several proinflammatory molecules involved in lymphocyte
362 migration and activation, including CCL17 in individuals with high CAA pre-vaccination suggesting a
363 coordinated immune response in instances of high worm burden. Higher levels of CCL17 and sIL-2R
364 showed negative associations with HepB titers in cases of high worm burden, identifying these two
365 molecules as potential biomarkers for inefficient antibody development. CCL17 has been shown to play a
366 key role in recruiting CCR4-expressing T helper and regulatory cells during inflammation (34-36, 38).
367 Furthermore, Wirnsberger and colleagues specifically show that IL-4 induces the expression of CCL17
368 (56), and we observed higher levels of IL-4 in individuals with high CAA post-vaccination (data not
369 shown) suggesting IL-4 may be playing a role in driving and sustaining the CCL17 responses observed.
370 While T helper 1 and 2 responses, are predominant in Schistosomiasis (14), these chronically skewed
371 environments have been known to be antagonistic to Tfh-B cell interactions that are important for
372 inducing antigen-specific antibody responses (18, 19, 40). Furthermore, alterations in innate immune
373 function in *Schistosoma* infection observed in our cohort, may potentially play a role in these shifts in
374 these cytokine levels; and previous models have also shown that elevation of T-helper cytokines in *S.*
375 *mansoni* infection correlate specifically with lower vaccine-specific responses to immunization against
376 *Mycobacterium bovis* (BCG) (21), HepB and tetanus toxoid (26).

377 Several Tfh cell subsets involved in antibody induction during infection and vaccination,
378 including cTfh cells in the periphery, play a key role the generation of high-affinity antibody-producing
379 plasma cells and memory B cells (39). We also now know that changes observed in cTfh profiles are
380 known to reflect the cytokine microenvironment, and specific cTfh subpopulations are known to drive B
381 cell class switching (57). We demonstrated that individuals with high CAA had lower cTfh1 and -2 cells
382 pre-vaccination, which was sustained post-vaccination for cTfh1 and cTfh17 cells in this group. More

383 specifically, a positive association between HepB-specific memory CD4⁺ T cell responses and HepB-
384 specific antibody production was observed. These data highlight the vital role of HepB-specific memory
385 CD4⁺ T helper cells in driving antibody responses, and that changes in this compartment directly
386 influences vaccine responses. In parallel, we also reported higher frequencies of in Foxp3⁺Tregs in
387 individuals with high CAA post-vaccination, suggesting a polarization towards higher frequencies of
388 Tregs. These data strongly suggest that in instances of high worm burden, robust regulatory responses can
389 be induced by key pro-Treg cytokines pre-vaccination, such as CCL17 (36, 37), and other cytokines such
390 as IL-2 which we also observe to be elevated pre-vaccination (S1E Fig), can inhibit Tfh responses (58).
391 We believe this environment at baseline can dictate varied changes to the T cell profile and kinetics post-
392 vaccination and skew the ratio of Tregs: cTfh cells when there is a high worm burden. Interestingly, it has
393 also been shown that the spleen is a major source of Tregs in hepatosplenic schistosomiasis (59), and we
394 can hypothesize that higher frequencies of Tregs in this condition, could contribute to a diminished
395 vaccine-induced response.

396 In support of our findings, Yin et. al. recently reported that lower responders to HepB vaccination
397 had lower frequencies of cTfh cells and antibody-secreting plasmablasts (42); and Musaigwa and
398 colleagues describe that *S. mansoni* infection specifically induces cell death in bone marrow plasmablasts
399 and plasma cells (60). We show in addition to a lower frequency of cTfh cells in individuals with high
400 CAA, a significant increase in activated B cells but a reduction in proliferating (antigen-specific) ASCs,
401 ASCs expressing IgG and IgA, and that IgA⁺ASCs positively correlate with HepB titers. In addition to
402 these data, we see a significant reduction in TLR9-induced IgA levels post-vaccination. In combination,
403 these results point to a direct role for high worm burden environments pre-vaccination in influencing
404 changes in the immune landscape polarizing it away from cTfh and B cell responses which would hamper
405 vaccine-specific antibody production post-vaccination. Induction of IgA is a significant and desirable aim
406 of vaccination for its advantageous role in mucosal responses and has been proven to be associated with
407 protection effects post-vaccination (45, 61). We have also previously shown that changes to the cytokine
408 microenvironment, particularly hyperinflammation, drives sustained dysregulation of the Tfh-B cell

409 interaction and hence B cell function (40, 41). Together these results emphasize that for successful
410 vaccination, an overall efficient Tfh and B cell response is required.

411 Innate responses play critical role in shaping the adaptive immune response to vaccines. We show
412 the importance of monocyte function in innate immune responses and desired vaccine responses to HepB.
413 While our analysis showed higher levels of several innate proinflammatory cytokines in the plasma of
414 individuals with high CAA, we did not observe an association between frequencies of monocyte
415 populations and *S. mansoni* infection. However, after stimulation with a viral TLR 7/8 ligand, we show
416 that the levels of induced cytokines varied with *S. mansoni* infection, evidenced by mixed responses pre-
417 and 12 days post-vaccination. These findings give some indication on how pro-inflammatory innate
418 environments could direct the disruption of efficient vaccine-specific responses during *Schistosoma*
419 infection. Furthermore, these results suggest that innate cells are playing a distinctive functional role in
420 changing this early cytokine/chemokine microenvironment, which we know impacts overall adaptive
421 immunity. Specifically, induction of CXCL10 (IP-10), which plays a crucial role in the activation and
422 recruitment of leukocytes and monocytes, promoting DC maturation and inducing protective T cell
423 responses (47, 48), was decreased in individuals with high worm burden pre-vaccination. CXCL10 has
424 been shown to promote the recruitment of CXCR3⁺ cells, which not only include activated T and B cells
425 (62, 63), but also the B-helper Tfh cells important in efficient responses to infection and vaccination (64-
426 66). A CXCL10- inclusive signature was also associated with effective immune responses to a SARS-
427 CoV-2 vaccine after the 1st vaccination (67), and recent vaccination studies also highlighted a link
428 between CXCL10 levels in the serum and innate responses associated with increased vaccine-specific
429 antibody titers (68, 69). Our data, combined with other studies, highlight a vital role for CXCL10 in
430 modulating the early response to vaccination.

431 Notably, it has been demonstrated that deworming can enhance the host immune response to
432 vaccination (25), and some studies have shown that PZQ treatment can partially restore vaccine-induced
433 immune responses (60, 70). While all enrolled individuals in this current study were treated with PZQ at
434 D12 post-vaccination (Fig 1), it is possible that *Schistosoma*-related effects on baseline immune responses

435 may have already occurred. Furthermore, the rate of reinfection and the extent to which the initial
436 infection was cleared, is also unknown; and as this study also indicates that several proinflammatory
437 cytokines at baseline remain elevated at month 12 post-vaccination, it is possible that individuals with a
438 higher baseline CAA concentration get more reinfections with time, creating a cycle of high CAA
439 concentration driving inefficient immune responses to secondary antigen. Despite these limitations, we
440 observed differences in vaccine-induced responses in individuals with varying pre-vaccinated levels of
441 CAA, irrespective of reported PQZ treatment. A similar observation was seen in an animal study of
442 chronic schistosomiasis and HIV vaccination where schistosomiasis suppressed vaccine responses, and
443 this was maintained regardless of anti-helminth treatment (71). While we know anti-helminth treatment is
444 effective at clearing worms, results suggest that *Schistosoma* infection in this study is associated with
445 irreversible immunomodulatory effects that can influence a host's response to unrelated antigen, such as
446 those in vaccines.

447 In this study, we did not evaluate for transgenerational exposure to *Schistosoma*. Previous studies
448 have shown that parasite antigen and maternal antibodies can transfer from mothers to babies in utero and
449 during breastfeeding (72), and some studies have showed lower vaccine responses in the newborns of
450 *Schistosoma*-infected mothers (73-75). These observations highlight the potential for different baseline
451 immune responses in individuals with transgenerational exposure to *Schistosoma* infection and its effect
452 on vaccine responses needs further investigation. It is also likely that some individuals are genetically
453 more susceptible to *Schistosoma* and related hepatic fibrosis than others (76), and further understanding is
454 needed on how susceptibility and high worm load may contribute to how these individuals mount
455 effective vaccine responses. In this study we adjusted for age and sex but people with *Schistosoma* may
456 be more likely to have other exposures (including other worm species, different microbiome) (77), which
457 might influence vaccine response.

458 In summary, high worm burden in *S. mansoni* infection is associated with the dysregulation of
459 vaccine-induced responses by the cooperation of key cytokines/chemokines that lead to elevated
460 inflammation, and lower levels of cytokines that promote the frequency and function of innate and

461 adaptive immune subsets important in generating vaccine-specific antibodies. Furthermore, a high CCL17
462 and low CXCL10-inclusive cytokine/chemokine signature pre-vaccination in instances of high worm
463 burden, is also identified. The results from our study could be applied to instruct ongoing and future
464 projects to benefit vaccination programs in *Schistosoma*- and other helminth- endemic communities,
465 particularly in the design of studies that address specific hypotheses such as recently published study
466 protocols from Nkurunungi and colleagues which describe the effect of a more intensive intervention with
467 anti-helminth treatment on vaccine responses in adolescents in Uganda (78, 79).

468

469 **Methods**

470 **Study participants and design**

471 Healthy adult volunteers who were enrolled in this study were one-arm of a community-based
472 prospective investigation that took place in fishing communities located in Entebbe, Uganda, called the
473 Stimulated Vaccine Efficacy Trial (SiVET). SiVET was set up to identify populations and assess the
474 implementation of efficacy trial procedures. Hepatitis B and typhoid vaccines were selected as simulated
475 vaccines due to the potential benefit to the fishing communities. Participants aged 18 to 49 years, males
476 and non-pregnant females were enrolled starting in 2015 from one mainland lakeshore fishing community
477 and one island community along Lake Victoria, in Wakiso district. (S1 Table). Inclusion criteria
478 encompassed HIV-uninfected, negative Hep B surface antigen (HbsAg) and core antibody tests,
479 capability, and willingness to provide written informed consent to receive HBV vaccine, and consent for
480 follow-up leading up to 12 months after the first study immunization. Volunteers were not prescreened for
481 active malaria and latent TB infections. Samples from 75 volunteers were available to be used for this
482 present sub-study with the objective to explore predictors of immune responses, (including parasite
483 burden, microbiome, effect of diet on microbiome) and to explore novel methods to identify predictors of
484 vaccine response and pathways activated in effective vaccine immune responses. Adults were screened up
485 to 6 weeks before the first study injection of the Hepatitis B vaccine ENGERIX-B (GlaxoSmithKline
486 Biologicals, derived from recombinant subunit Hepatitis B surface antigen adsorbed on aluminum

487 hydroxide) followed by two booster doses given at months 1 and 6 (Fig 1). Doses were given
488 intramuscularly in the deltoid muscle at 1mL volume containing 20 µg of the vaccine. Whole blood and
489 plasma were collected pre-vaccination (D0), post-1st injection (D3, D7, and D12), and post-booster
490 injections on the day the infections were administered (M1 and M6) (Fig 1). Volunteers were treated at
491 day 12 with Praziquantel (PZQ) as appropriate, for egg counts detected in stool samples at enrollment,
492 D3, and/or D7 (Fig 1). *Schistosoma*-infected participants received 40mg/kg body weight single dose
493 (average 2.4 g) of PZQ.

494

495 **Treatment of *S. mansoni*-infected enrolled individuals**

496 Stool samples were collected from enrollees' pre-vaccination (D0), prior to the first dose of the
497 HepB vaccine, and at D3 and D7 post-vaccination. *Schistosoma* egg counts were subsequently conducted
498 and if stool sample/s were positive, PZQ treatment was administered at D12 post-vaccination. Egg count
499 results were available within one week, after which any infected individuals were treated.

500

501 **Circulating anodic antigen (CAA) assay**

502 The circulating anodic antigen assay (CAA) was performed pre-vaccination (Day 0) on serum
503 samples from enrolled participants to reveal ongoing *Schistosoma* infection (29-32). Human negative
504 serum (Sanquin, blood donors, the Netherlands) was spiked with a known concentration of CAA and
505 dilutions made up to eight standard points to provide an appropriate standard series. An extra negative
506 serum sample was included as a duplicate negative control. Samples were evaluated using the SCAA500
507 protocol with a lower limit of detection threshold of 3pg/mL; 500 µL serum and standards were extracted
508 with an equal volume of 4% w/v trichloroacetic acid (TCA; Merck Life Science NV, the Netherlands),
509 vortexed and incubated at ambient temperature for five minutes. Thereafter, samples and standards were
510 briefly vortexed and spun at 13000g for five minutes and 0.5 mL of clear supernatant was concentrated to
511 20 µL using Amicon Ultra-0.5 Centrifugal Filter Units devices with a molecular weight cut-off of 10 kDa
512 (Merck Life Science N.V., the Netherlands). Note, for samples with insufficient serum volumes the

513 SCAA20 test format was used which requires only 20uL serum and no concentration step but has a lower
514 limit of detection threshold of 30pg/mL. The resulting TCA soluble fraction (20µL) was added to wells
515 containing 100 ng dry UCP particles (80) (400 nm Y₂O₂S:Yb³⁺,Er³⁺) coated with mouse monoclonal anti-
516 CAA antibodies (32) hydrated with 100 mL of high salt lateral flow buffer (HSFS: 200 mM Tris pH8,
517 270 mM NaCl, 0.5% (v/v) Tween-20, 1% (w/v) BSA. After incubated for one hour at 37°C while shaking
518 at 900rpm the CAA lateral flow strips (32) were placed in the wells, and samples allowed to flow. The
519 strips were then dried overnight and analyzed using an Upcon reader (Labrox Oy, Turku, Finland). The
520 test line signals (T; relative fluorescent units, peak area) were normalized to the flow control signals (FC)
521 of the individual strips and the results expressed as Ratio value (R=T/FC).

522

523 **Whole blood processing and sample storage**

524 PBMCs isolation/storage: Whole Blood collected in NaHeparin tube (BD, NJ, USA) was layered
525 over 20ml of Histopaque (Sigma-Aldrich, Darmstadt, Germany) and centrifuged at 400g for 40 minutes at
526 room temperature with no centrifuge brakes. Lymphocytes, platelets, and monocytes found at the plasma-
527 separating medium interface (buffy coat) were recovered and washed in Hanks Balanced Salt solution to
528 remove contaminating platelets, separation media and plasma. The resulting PBMCs (lymphocytes and
529 monocytes) were resuspended in complete RPMI media (RPMI 1640 media supplemented with 10% Fetal
530 Bovine Serum (FBS), 10mM Hepes buffer, 2mM L-glutamine, 1mM sodium pyruvate and 1X penicillin-
531 streptomycin) for counting and concentrated at 10million cells/mL/ vial in FBS with 10% DMSO, frozen
532 down using a rate-controlled freezer and stored in liquid nitrogen.

533 **Serum separation:** Specific vacutainers for serum (SST, Plymouth UK) were invert twice to mix
534 blood and then centrifuged at 1200 g for 10 minutes at room temperature with maximum acceleration and
535 brake after which aliquots into pre-labeled cryovials were made and stored at below -70°C.

536 **Plasma separation:** Plasma from the separation tube of PBMCs was harvested and then
537 centrifuged at 1800 g for 20 minutes at room temperature with maximum acceleration and brake after

538 which aliquots into pre-labeled cryovials without disturbing the platelet pellet at the bottom of the tube
539 and stored at below -70°C .

540

541 **Hepatitis B antibody testing**

542 Each serum sample was assayed at screening using three different HBV infection tests for:
543 Hepatitis B surface antigen (HbsAg), Hepatitis B core antibody (anti-HBc), and Hepatitis B surface
544 antibody (anti-HBs). The HbsAg and antiHBc antibodies were tested for using the VIDAS HbsAg Ultra
545 and VIDAS anti-HBc Total II (Biomerieux SA, France) kits respectively on the MinVidas analyzer. The
546 anti-HBs testing was done using the Cobas e 411 analyzer (Roche Diagnostics, Mannheim, Germany).
547 The anti-HBs titer cut off value was 10IU/L. All three tests were used only at screening to differentiate
548 between possible past exposure from active infection, and to ensure only HepB-negative individuals were
549 recruited and administered the vaccine. Measurement of anti-HBs antibody was conducted for all
550 subsequent follow-up visits.

551

552 **PBMC culture**

553 PBMCs from non-infected and *S. mansoni*-infected individuals pre-vaccination and post-
554 vaccination were thawed and rested for 3 hours before being placed into culture. Samples were used for
555 ex-vivo immunostaining and flow cytometry analysis, and for TLR stimulation assays. PBMCs were
556 suspended in RPMI medium supplemented with L-glutamine (Corning Cellgro, Manassas, VA, USA),
557 10% FBS and 1 X [50 U] penicillin-streptomycin (Invitrogen, Carlsbad, CA, USA) (R10F). 1×10^6 cells
558 were added to 5-ml polypropylene tubes for CLO97 stimulation (Imidazoquinoline Compound; TLR7/8
559 agonist) (Invivogen, San Diego, CA, USA), and 0.5×10^6 cells added to the wells of 96-well U-bottom
560 plates for CpG-ODN 2006 stimulation (TLR9 agonist) (Invivogen). Optimal concentration for CLO97
561 stimulation was selected as previously described (81). CpG-ODN 2006 was titrated on CFSE-labeled
562 PBMCs, and optimal TLR9 activity assessed on proliferating CD19⁺ cells by flow cytometry. Cells were
563 allowed to rest at 37°C under a 5% CO_2 atmosphere for 3 hours prior to addition of TLR agonists at the

564 following concentrations: CLO97 (0.5ug/ml) and CpG (1ug/ml). Cells were cultured also at 37°C under a
565 5% CO² atmosphere for 18hrs (CLO97), and 7 days (CpG-ODN 2006). After culture, PBMCs were
566 collected and washed in preparation for analysis by multiplex immunoassays or flow cytometry. For HBV
567 peptide stimulation, PBMCs were first labeled with CFSE using a Cell Trace™ CFSE cell proliferation
568 kit (ThermoFisher Scientific, Waltham, MA, USA), and rested for 3 hours in the conditions described
569 above. In a 96-well deep well plate (USA Scientific, Ocala, FL, USA), 2 x 10⁶ cells in 1mL RPMI
570 medium supplemented with 8% human serum (Access Biologicals, Vista, CA, USA), 1% penicillin-
571 streptomycin and 10ng/mL IL-2 (Miltenyi Biotec, Auburn, CA, USA) (R8H-IL-2) were stimulated with
572 either Pepmix™ HBV (Large envelope protein) (JPT Peptide Technologies, Berlin, Germany) at 1ug/mL
573 or control (R8H-IL-2 with 0.2% DMSO) on Day 1 and cultured in the conditions described above. On
574 Day 3, cells were supplemented with fresh R8H-IL-2 by half media replacement; and on Day 6, PBMCs
575 were collected and washed in preparation for measurement of immune recall responses by flow
576 cytometry.

577

578 **Cytokine and chemokine analysis (multiplex immunoassay)**

579 Plasma collected from whole blood and supernatant collected from stimulated PBMCs were
580 analyzed for chemokines/cytokines and Ig isotypes using magnetic bead multiplex assays. The following
581 human analyte premixed panels were used: Bio-Plex human chemokine panel (Bio-Rad, Hercules, CA,
582 USA): I-309 (CCL1), MCP-1 (CCL2), MIP-1 α (CCL3), MCP-3 (CCL7), MCP-2 (CCL8), Eotaxin
583 (CCL11), MCP-4 (CCL13), MIP-1 α (CCL15), TARC (CCL17), MIP-3 β (CCL19), 6Ckine (CCL21),
584 MIP-3 α (CCL20), MDC (CCL22), MPIF-1 (CCL23), Eotaxin-2 (CCL24), TECK (CCL25), Eotaxin-3
585 (CCL26), CTACK (CCL27), GM-CSF, GRO- α (CXCL1), GRO- β (CXCL2), ENA-78 (CXCL5), GCP-2
586 (CXCL6), MIG (CXCL9), IP-10 (CXCL10), I-TAC (CXCL11), SDF-1A+ β (CXCL12), BCA-1
587 (CXCL13), SCYB16 (CXCL16), Fractalkine (CX3CL1), MIF, IL-1 β , IL-2, IL-4, IL-6, IL-8, IL-10, IL-
588 16, TNF- α , and IFN- γ . Custom ProcartaPlex 34-plex (ThermoFisher Scientific): APRIL, BAFF, CD30,
589 CD40L, G-CSF, IFN-A, IL-12P70, IL-13, IL-15, IL-16, IL-17A, IL-18, IL-1A, IL-20, IL-21, IL-22, IL-

590 23, IL-27, IL-2R, IL-3, IL-31, IL-5, IL-7, IL-9, LIF, M-CSF, TNF-R2, TNF-B, TRAIL, TSLP, TWEAK,
591 VEGF-A, IFNB, and IL-29/IFN-lambda1. Bio-Plex human isotype panel (Bio-Rad): IgM, IgA, IgG1,
592 IgG2, IgG3, IgG4. IgE was measured using Bio-Plex human IgE isotype assay (Bio-Rad). The
593 manufacturer's protocol was followed. Data was acquired on a Bio-Plex 200 system (using bead regions
594 defined in the protocol) and analyzed with the Bio-Plex Manager 6.1 software (Bio-Rad).

595

596 **Flow cytometry analysis of PBMCs**

597 For ex-vivo analysis, 1×10^6 PBMCs per well were incubated with Fixable aqua viability stain
598 405 (ThermoFisher Scientific) to discriminate dead from live cells then stained with antibody panels
599 described (S8 and S9 Tables). To detect intracellular expression of markers, cells were fixed and
600 permeabilized using the Foxp3/Transcription factor staining buffer set (ThermoFisher Scientific) and
601 immunostained using FOXP3-FITC (clone, PCH101) (ThermoFisher Scientific) (S8 Table) and KI67-
602 FITC (BD Biosciences, San Jose, CA, USA) (S9 Table). Following HBV peptide stimulation, PBMCs
603 were stained with the surface antibody panel described (S10 Table), then stained with 7-AAD (BD
604 Biosciences) for 10 minutes prior to analysis to discriminate dead from live cells. Flow cytometry
605 measurements were made on a BD LSRFortessa™ (BD Biosciences) and collected data analyzed using
606 FlowJo software version 10.7.1 (BD).

607

608 **Antibody-dependent cellular phagocytosis (ADCP) assay**

609 An antibody-dependent cellular phagocytosis (ADCP) assay to investigate monocyte function
610 was conducted. HbsAg was biotinylated using an EZ-Link™ Sulfo-NHS-LC-Biotinylation Kit
611 (ThermoFisher Scientific) and coupled to FluoSpheres™ NeutrAvidin™-Labeled Microspheres
612 (ThermoFisher Scientific). To form immune complexes, antigen-coupled beads were incubated for 2
613 hours at 37°C with 1:25 diluted serum samples and then washed to remove unbound immunoglobulin.
614 After washing, immune complexes were incubated for 16-18 hours with a monocyte cell line, THP-1 cells
615 [25,000 THP-1 cells per well at a concentration of 1.25×10^5 cells/ml in RPMI (ThermoFisher Scientific)

616 + 10% FBS (Sigma-Aldrich), and following incubation, cells were fixed with 4% paraformaldehyde (Poly
617 Scientific R&D, Bay Shore, NY, USA). Percentage of fluorosphere positive cells was analyzed on a
618 LSRII flow cytometer (BD Biosciences). The phagocytosis score was defined.

619

620 **Antibody subclass and Fc receptor binding**

621 HbSAg-specific antibody subclass titers and Fc receptor binding profiles were analyzed with a
622 custom multiplex Luminex assay as described previously (82). In brief, HbSAg was coupled to magnetic
623 Luminex beads (Luminex Corp, TX, USA). Coupled beads were incubated with diluted serum samples,
624 washed, and IgG subclasses detected with a 1:100 diluted PE-conjugated secondary antibody for IgG1
625 (clone: HP6001; Southern Biotech, AL, USA). For the Fc γ R binding, a respective PE-streptavidin
626 (Agilent Technologies, Santa Clara, CA, USA) coupled recombinant and biotinylated human Fc γ R
627 protein was used as a secondary probe.

628

629 **Statistics**

630 Statistical inference evaluating the differences of HepB titers between non-infected versus low
631 CAA, non-infected versus high CAA and low CAA versus high CAA was determined using Wilcoxon
632 rank-sum test. Wilcoxon rank-sum tests were performed on non-infected vs. low CAA, or non-infected
633 vs. high CAA, or low CAA vs. high CAA within each time point for plasma Luminex assays, and ex-vivo
634 flow cytometry analysis. Pairwise Wilcoxon signed rank test were performed on untreated vs. treated for
635 each non-infected, or low CAA, or high CAA for CpG, HBV-LEP and CLO97 stimulation assays; and
636 within the treated groups, a Wilcoxon rank-sum test was conducted on non-infected vs. low CAA, or non-
637 infected vs. high CAA, or low CAA vs. high CAA. Linear regression analyses were adjusted for sex (no
638 significant association between age and HepB titers) and student t-tests were used to evaluate for the
639 significance of the association. Sensitivity analyses were performed using the R package sensemakr (83)
640 used to assess the robustness of the results of the linear regression analysis to an unobserved confounding

641 variable. Benjamini-Hochberg adjustment was used to control for multiple testing for each assay. $P \leq 0.05$
642 was considered significant for all analyses.

643

644 **Study approval**

645 Informed consent was obtained from all participants prior to being enrolled in the studies. All
646 studies were approved by the Uganda Virus Research Institute Research Ethics Committee, reference
647 number GC/127/15/07/439 and the Uganda National Council of Science and Technology, reference
648 number HS 1850.

649

650 **Author contributions**

651 RM, TM, and SF share first authorship. RM and TM are first and second co-authors respectively,
652 as they conceptualized, designed, and performed experiments, analyzed data, and wrote the manuscript.
653 SF is the third co-author and analyzed data and wrote the manuscript. AK, NK, A Nanvubya, PK, BSB
654 and YM designed the SiVET clinical study. AK, AE, PK, JKL and BSB conceptualized the SiVET study.
655 YB, JKL, GC, GA, EM, BO, TN, IN, A Namuniina, AS, JM, PKK, VMB, BSB, NK, JN, WS, CJDD, PB
656 and MO performed experiments and analyzed data. PLAMC and GJVD designed clinical assays and
657 PLAMC edited the manuscript. EM, BO, TN, IN, AN, AS, JM, PKK, and NK managed enrollee
658 recruitment and participation in the study. PF, MAP, AME, and RPS provided conceptual advice and
659 edited the manuscript. EKH conceptualized experiments and wrote the manuscript. All authors reviewed
660 and approved the manuscript. RM and EKH had final responsibility for the decision to submit for
661 publication.

662

663 **Acknowledgements**

664 This work was supported by NIH funding as part of Human Immune Project Consortium (HIPC)
665 to EKH and RPS #U19 AI128910. The SiVET was supported by a grant from the United States Agency

666 for International Development (USAID) [USAID reference number AID-OAA-A-16-00032]. The
667 contents are the responsibility of the authors and does not necessarily reflect the views of USAID or the
668 United States Government. We are grateful to the study participants, and healthcare and research staff
669 from the Immunomodulation and Vaccines Programme and the Pathogen Genomics Phenotype and
670 Immunity Programme at the MRC/UVRI and LSHTM Uganda Research Unit, the UVRI-IAVI HIV
671 Vaccine Program at the College of Health Sciences at Makerere University, Kampala-Uganda, and the
672 International AIDS Vaccine initiative, for the invaluable contribution to this study.

673

674 **References**

675

- 676 1. Pollard AJ, Bijker EM. A guide to vaccinology: from basic principles to new
677 developments. *Nat Rev Immunol*. 2021;21(2):83-100.
- 678 2. Zimmermann P, Curtis N. Factors That Influence the Immune Response to Vaccination.
679 *Clin Microbiol Rev*. 2019;32(2).
- 680 3. Driciru E, Koopman JPR, Cose S, Siddiqui AA, Yazdanbakhsh M, Elliott AM, et al.
681 Immunological Considerations for Schistosoma Vaccine Development: Transitioning to Endemic
682 Settings. *Front Immunol*. 2021;12:635985.
- 683 4. Nono JK, Kamdem SD, Musaigwa F, Nnaji CA, Brombacher F. Influence of
684 schistosomiasis on host vaccine responses. *Trends Parasitol*. 2022;38(1):67-79.
- 685 5. Ssali A, Pickering L, Nalwadda E, Mujumbusi L, Seeley J, Lambertson PHL.
686 Schistosomiasis messaging in endemic communities: Lessons and implications for interventions
687 from rural Uganda, a rapid ethnographic assessment study. *PLoS Negl Trop Dis*.
688 2021;15(10):e0009893.
- 689 6. Loewenberg S. Uganda's struggle with schistosomiasis. *Lancet*. 2014;383(9930):1707-8.
- 690 7. World Health Organization. Assessing the Efficacy of Anthelmintic Drugs against
691 Schistosomiasis and Soil-Transmitted Helminthiasis . Geneva, Switzerland: World Health
692 Organization. <https://apps.who.int/iris/handle/10665/79019> Accessed on 06/16/2022. 2013.
- 693 8. Omar HH. Impact of chronic schistosomiasis and HBV/HCV co-infection on the liver:
694 current perspectives. *Hepat Med*. 2019;11:131-6.
- 695 9. Bwogi J, Braka F, Makumbi I, Mishra V, Bakamutumaho B, Nanyunja M, et al. Hepatitis
696 B infection is highly endemic in Uganda: findings from a national serosurvey. *Afr Health Sci*.
697 2009;9(2):98-108.
- 698 10. Kafeero HM, Ndagire D, Ocamo P, Kudamba A, Walusansa A, Sendagire H. Prevalence
699 and predictors of hepatitis B virus (HBV) infection in east Africa: evidence from a systematic
700 review and meta-analysis of epidemiological studies published from 2005 to 2020. *Arch Public*
701 *Health*. 2021;79(1):167.

- 702 11. Kitandwe PK, Muyanja E, Nakaweesa T, Nanvubya A, Ssetaala A, Mpendo J, et al.
703 Hepatitis B prevalence and incidence in the fishing communities of Lake Victoria, Uganda: a
704 retrospective cohort study. *BMC Public Health*. 2021;21(1):394.
- 705 12. Pattyn J, Hendrickx G, Vorsters A, Van Damme P. Hepatitis B Vaccines. *J Infect Dis*.
706 2021;224(12 Suppl 2):S343-S51.
- 707 13. Walayat S, Ahmed Z, Martin D, Puli S, Cashman M, Dhillon S. Recent advances in
708 vaccination of non-responders to standard dose hepatitis B virus vaccine. *World J Hepatol*.
709 2015;7(24):2503-9.
- 710 14. Kamdem SD, Moyou-Somo R, Brombacher F, Nono JK. Host Regulators of Liver
711 Fibrosis During Human Schistosomiasis. *Front Immunol*. 2018;9:2781.
- 712 15. Angeles JMM, Mercado VJP, Rivera PT. Behind Enemy Lines: Immunomodulatory
713 Armamentarium of the Schistosome Parasite. *Front Immunol*. 2020;11:1018.
- 714 16. Zheng B, Zhang J, Chen H, Nie H, Miller H, Gong Q, et al. T Lymphocyte-Mediated
715 Liver Immunopathology of Schistosomiasis. *Front Immunol*. 2020;11:61.
- 716 17. Lundy SK, Lukacs NW. Chronic schistosome infection leads to modulation of granuloma
717 formation and systemic immune suppression. *Front Immunol*. 2013;4:39.
- 718 18. Vinuesa CG, Linterman MA, Yu D, MacLennan IC. Follicular Helper T Cells. *Annu Rev*
719 *Immunol*. 2016;34:335-68.
- 720 19. Crotty S. T Follicular Helper Cell Biology: A Decade of Discovery and Diseases.
721 *Immunity*. 2019;50(5):1132-48.
- 722 20. Su Z, Segura M, Stevenson MM. Reduced protective efficacy of a blood-stage malaria
723 vaccine by concurrent nematode infection. *Infect Immun*. 2006;74(4):2138-44.
- 724 21. Elias D, Akuffo H, Pawlowski A, Haile M, Schon T, Britton S. *Schistosoma mansoni*
725 infection reduces the protective efficacy of BCG vaccination against virulent *Mycobacterium*
726 *tuberculosis*. *Vaccine*. 2005;23(11):1326-34.
- 727 22. Chen L, Liu WQ, Lei JH, Guan F, Li MJ, Song WJ, et al. Chronic *Schistosoma*
728 *japonicum* infection reduces immune response to vaccine against hepatitis B in mice. *PLoS One*.
729 2012;7(12):e51512.
- 730 23. Nono JK, Kamdem SD, Netongo PM, Dabee S, Schomaker M, Oumarou A, et al.
731 Schistosomiasis Burden and Its Association With Lower Measles Vaccine Responses in School
732 Children From Rural Cameroon. *Front Immunol*. 2018;9:2295.
- 733 24. Tweyongyere R, Nassanga BR, Muhwezi A, Odongo M, Lule SA, Nsubuga RN, et al.
734 Effect of *Schistosoma mansoni* infection and its treatment on antibody responses to measles
735 catch-up immunisation in pre-school children: A randomised trial. *PLoS Negl Trop Dis*.
736 2019;13(2):e0007157.
- 737 25. Song WJ, Cheng YL, Liu LZ, Kong Z, Hu S, Liu K, et al. [Impact of chronic
738 schistosomiasis japonica on the protective immunity induced by vaccine against hepatitis B
739 virus]. *Zhongguo Ji Sheng Chong Xue Yu Ji Sheng Chong Bing Za Zhi*. 2005;23(3):163-5.
- 740 26. Riner DK, Ndombi EM, Carter JM, Omondi A, Kittur N, Kavere E, et al. *Schistosoma*
741 *mansoni* Infection Can Jeopardize the Duration of Protective Levels of Antibody Responses to
742 Immunizations against Hepatitis B and Tetanus Toxoid. *PLoS Negl Trop Dis*.
743 2016;10(12):e0005180.
- 744 27. Alan Wilson R, van Dam GJ, Kariuki TM, Farah IO, Deelder AM, Coulson PS. The
745 detection limits for estimates of infection intensity in schistosomiasis mansoni established by a
746 study in non-human primates. *Int J Parasitol*. 2006;36(12):1241-4.

- 747 28. van Dam GJ, Bogitsh BJ, van Zeyl RJ, Rotmans JP, Deelder AM. *Schistosoma mansoni*:
748 in vitro and in vivo excretion of CAA and CCA by developing schistosomula and adult worms. *J*
749 *Parasitol.* 1996;82(4):557-64.
- 750 29. Corstjens P, de Dood CJ, Knopp S, Clements MN, Ortu G, Umulisa I, et al. Circulating
751 Anodic Antigen (CAA): A Highly Sensitive Diagnostic Biomarker to Detect Active *Schistosoma*
752 Infections-Improvement and Use during SCORE. *Am J Trop Med Hyg.* 2020;103(1_Suppl):50-
753 7.
- 754 30. Corstjens P, Hoekstra PT, de Dood CJ, van Dam GJ. Utilizing the ultrasensitive
755 *Schistosoma* up-converting phosphor lateral flow circulating anodic antigen (UCP-LF CAA)
756 assay for sample pooling-strategies. *Infect Dis Poverty.* 2017;6(1):155.
- 757 31. Corstjens PL, De Dood CJ, Kornelis D, Fat EM, Wilson RA, Kariuki TM, et al. Tools for
758 diagnosis, monitoring and screening of *Schistosoma* infections utilizing lateral-flow based assays
759 and upconverting phosphor labels. *Parasitology.* 2014;141(14):1841-55.
- 760 32. Corstjens PL, van Lieshout L, Zuiderwijk M, Kornelis D, Tanke HJ, Deelder AM, et al.
761 Up-converting phosphor technology-based lateral flow assay for detection of *Schistosoma*
762 circulating anodic antigen in serum. *J Clin Microbiol.* 2008;46(1):171-6.
- 763 33. Corstjens PL, Nyakundi RK, de Dood CJ, Kariuki TM, Ochola EA, Karanja DM, et al.
764 Improved sensitivity of the urine CAA lateral-flow assay for diagnosing active *Schistosoma*
765 infections by using larger sample volumes. *Parasit Vectors.* 2015;8:241.
- 766 34. Imai T, Nagira M, Takagi S, Kakizaki M, Nishimura M, Wang J, et al. Selective
767 recruitment of CCR4-bearing Th2 cells toward antigen-presenting cells by the CC chemokines
768 thymus and activation-regulated chemokine and macrophage-derived chemokine. *Int Immunol.*
769 1999;11(1):81-8.
- 770 35. Lieberam I, Forster I. The murine beta-chemokine TARC is expressed by subsets of
771 dendritic cells and attracts primed CD4+ T cells. *Eur J Immunol.* 1999;29(9):2684-94.
- 772 36. Mizukami Y, Kono K, Kawaguchi Y, Akaike H, Kamimura K, Sugai H, et al. CCL17 and
773 CCL22 chemokines within tumor microenvironment are related to accumulation of Foxp3+
774 regulatory T cells in gastric cancer. *Int J Cancer.* 2008;122(10):2286-93.
- 775 37. Sharma A, Rudra D. Emerging Functions of Regulatory T Cells in Tissue Homeostasis.
776 *Front Immunol.* 2018;9:883.
- 777 38. Damoiseaux J. The IL-2 - IL-2 receptor pathway in health and disease: The role of the
778 soluble IL-2 receptor. *Clin Immunol.* 2020;218:108515.
- 779 39. Morita R, Schmitt N, Bentebibel SE, Ranganathan R, Bourdery L, Zurawski G, et al.
780 Human blood CXCR5(+)CD4(+) T cells are counterparts of T follicular cells and contain
781 specific subsets that differentially support antibody secretion. *Immunity.* 2011;34(1):108-21.
- 782 40. Cubas R, van Grevenynghe J, Wills S, Kardava L, Santich BH, Buckner CM, et al.
783 Reversible Reprogramming of Circulating Memory T Follicular Helper Cell Function during
784 Chronic HIV Infection. *J Immunol.* 2015;195(12):5625-36.
- 785 41. Muir R, Metcalf T, Tardif V, Takata H, Phanuphak N, Kroon E, et al. Altered Memory
786 Circulating T Follicular Helper-B Cell Interaction in Early Acute HIV Infection. *PLoS Pathog.*
787 2016;12(7):e1005777.
- 788 42. Yin M, Xiong Y, Liang D, Tang H, Hong Q, Liu G, et al. Circulating Tfh cell and subsets
789 distribution are associated with low-responsiveness to hepatitis B vaccination. *Mol Med.*
790 2021;27(1):32.

- 791 43. Ellebedy AH, Jackson KJ, Kissick HT, Nakaya HI, Davis CW, Roskin KM, et al.
792 Defining antigen-specific plasmablast and memory B cell subsets in human blood after viral
793 infection or vaccination. *Nat Immunol.* 2016;17(10):1226-34.
- 794 44. Colley DG, Secor WE. Immunology of human schistosomiasis. *Parasite Immunol.*
795 2014;36(8):347-57.
- 796 45. Boyaka PN. Inducing Mucosal IgA: A Challenge for Vaccine Adjuvants and Delivery
797 Systems. *J Immunol.* 2017;199(1):9-16.
- 798 46. Hopkins PA, Sriskandan S. Mammalian Toll-like receptors: to immunity and beyond.
799 *Clin Exp Immunol.* 2005;140(3):395-407.
- 800 47. Krathwohl MD, Anderson JL. Chemokine CXCL10 (IP-10) is sufficient to trigger an
801 immune response to injected antigens in a mouse model. *Vaccine.* 2006;24(15):2987-93.
- 802 48. Majumder S, Bhattacharjee S, Paul Chowdhury B, Majumdar S. CXCL10 is critical for
803 the generation of protective CD8 T cell response induced by antigen pulsed CpG-ODN activated
804 dendritic cells. *PLoS One.* 2012;7(11):e48727.
- 805 49. Yan Y, Chen R, Wang X, Hu K, Huang L, Lu M, et al. CCL19 and CCR7 Expression,
806 Signaling Pathways, and Adjuvant Functions in Viral Infection and Prevention. *Front Cell Dev*
807 *Biol.* 2019;7:212.
- 808 50. Stubbs VE, Power C, Patel KD. Regulation of eotaxin-3/CCL26 expression in human
809 monocytic cells. *Immunology.* 2010;130(1):74-82.
- 810 51. Kraynyak KA, Kutzler MA, Cisneros NJ, Khan AS, Draghia-Akli R, Sardesai NY, et al.
811 Systemic immunization with CCL27/CTACK modulates immune responses at mucosal sites in
812 mice and macaques. *Vaccine.* 2010;28(8):1942-51.
- 813 52. Dinarello CA. Overview of the IL-1 family in innate inflammation and acquired
814 immunity. *Immunol Rev.* 2018;281(1):8-27.
- 815 53. Saraiva M, O'Garra A. The regulation of IL-10 production by immune cells. *Nat Rev*
816 *Immunol.* 2010;10(3):170-81.
- 817 54. Barenbold O, Raso G, Coulibaly JT, N'Goran EK, Utzinger J, Vounatsou P. Estimating
818 sensitivity of the Kato-Katz technique for the diagnosis of *Schistosoma mansoni* and hookworm
819 in relation to infection intensity. *PLoS Negl Trop Dis.* 2017;11(10):e0005953.
- 820 55. Basch PF. *Schistosomes : development, reproduction, and host relations.* United States:
821 New York : Oxford University Press; 1991.
- 822 56. Wirnsberger G, Hebenstreit D, Posselt G, Horejs-Hoeck J, Duschl A. IL-4 induces
823 expression of TARC/CCL17 via two STAT6 binding sites. *Eur J Immunol.* 2006;36(7):1882-91.
- 824 57. Olatunde AC, Hale JS, Lamb TJ. Cytokine-skewed Tfh cells: functional consequences for
825 B cell help. *Trends Immunol.* 2021;42(6):536-50.
- 826 58. Qin L, Waseem TC, Sahoo A, Bieberkezhazi S, Zhou H, Galkina EV, et al. Insights Into
827 the Molecular Mechanisms of T Follicular Helper-Mediated Immunity and Pathology. *Front*
828 *Immunol.* 2018;9:1884.
- 829 59. Romano A, Hou X, Sertorio M, Dessein H, Cabantous S, Oliveira P, et al. FOXP3+
830 Regulatory T Cells in Hepatic Fibrosis and Splenomegaly Caused by *Schistosoma japonicum*:
831 The Spleen May Be a Major Source of Tregs in Subjects with Splenomegaly. *PLoS Negl Trop*
832 *Dis.* 2016;10(1):e0004306.
- 833 60. Musaiqwa F, Kamdem SD, Mpotje T, Mosala P, Abdel Aziz N, Herbert DR, et al.
834 *Schistosoma mansoni* infection induces plasmablast and plasma cell death in the bone marrow
835 and accelerates the decline of host vaccine responses. *PLoS Pathog.* 2022;18(2):e1010327.

- 836 61. Sheikh-Mohamed S, Isho B, Chao GYC, Zuo M, Cohen C, Lustig Y, et al. Systemic and
837 mucosal IgA responses are variably induced in response to SARS-CoV-2 mRNA vaccination and
838 are associated with protection against subsequent infection. *Mucosal Immunol.* 2022.
- 839 62. Griffith JW, Sokol CL, Luster AD. Chemokines and chemokine receptors: positioning
840 cells for host defense and immunity. *Annu Rev Immunol.* 2014;32:659-702.
- 841 63. Liu M, Guo S, Hibbert JM, Jain V, Singh N, Wilson NO, et al. CXCL10/IP-10 in
842 infectious diseases pathogenesis and potential therapeutic implications. *Cytokine Growth Factor*
843 *Rev.* 2011;22(3):121-30.
- 844 64. Locci M, Havenar-Daughton C, Landais E, Wu J, Kroenke MA, Arlehamn CL, et al.
845 Human circulating PD-1+CXCR3-CXCR5+ memory Tfh cells are highly functional and
846 correlate with broadly neutralizing HIV antibody responses. *Immunity.* 2013;39(4):758-69.
- 847 65. Bentebibel SE, Khurana S, Schmitt N, Kurup P, Mueller C, Obermoser G, et al.
848 ICOS(+)/PD-1(+)/CXCR3(+) T follicular helper cells contribute to the generation of high-avidity
849 antibodies following influenza vaccination. *Sci Rep.* 2016;6:26494.
- 850 66. Zhang J, Liu W, Wen B, Xie T, Tang P, Hu Y, et al. Circulating CXCR3(+) Tfh cells
851 positively correlate with neutralizing antibody responses in HCV-infected patients. *Sci Rep.*
852 2019;9(1):10090.
- 853 67. Bergamaschi C, Terpos E, Rosati M, Angel M, Bear J, Stellas D, et al. Systemic IL-15,
854 IFN-gamma, and IP-10/CXCL10 signature associated with effective immune response to SARS-
855 CoV-2 in BNT162b2 mRNA vaccine recipients. *Cell Rep.* 2021;36(6):109504.
- 856 68. Goncalves E, Bonduelle O, Soria A, Loulergue P, Rousseau A, Cachanado M, et al.
857 Innate gene signature distinguishes humoral versus cytotoxic responses to influenza vaccination.
858 *J Clin Invest.* 2019;129(5):1960-71.
- 859 69. Rechtien A, Richert L, Lorenzo H, Martrus G, Hejblum B, Dahlke C, et al. Systems
860 Vaccinology Identifies an Early Innate Immune Signature as a Correlate of Antibody Responses
861 to the Ebola Vaccine rVSV-ZEBOV. *Cell Rep.* 2017;20(9):2251-61.
- 862 70. Nono JK, Mpotje T, Mosala P, Aziz NA, Musaigwa F, Hlaka L, et al. Praziquantel
863 Treatment of *Schistosoma mansoni* Infected Mice Renders Them Less Susceptible to
864 Reinfection. *Front Immunol.* 2021;12:748387.
- 865 71. Dzihvhuho GA, Rehrl SA, Ndlovu H, Horsnell WGC, Brombacher F, Williamson AL, et
866 al. Chronic schistosomiasis suppresses HIV-specific responses to DNA-MVA and MVA-gp140
867 Env vaccine regimens despite antihelminthic treatment and increases helminth-associated
868 pathology in a mouse model. *PLoS Pathog.* 2018;14(7):e1007182.
- 869 72. Attallah AM, Ghanem GE, Ismail H, El Waseef AM. Placental and oral delivery of
870 *Schistosoma mansoni* antigen from infected mothers to their newborns and children. *Am J Trop*
871 *Med Hyg.* 2003;68(6):647-51.
- 872 73. Ghaffar YA, Kamel M, el-Sobky M, Bahnasy R, Strickland GT. Response to hepatitis B
873 vaccine in infants born to mothers with schistosomiasis. *Lancet.* 1989;2(8657):272.
- 874 74. Malhotra I, LaBeaud AD, Morris N, McKibben M, Mungai P, Muchiri E, et al. Cord
875 Blood Antiparasite Interleukin 10 as a Risk Marker for Compromised Vaccine Immunogenicity
876 in Early Childhood. *J Infect Dis.* 2018;217(9):1426-34.
- 877 75. Ondigo BN, Muok EMO, Oguso JK, Njenga SM, Kanyi HM, Ndombi EM, et al. Impact
878 of Mothers' Schistosomiasis Status During Gestation on Children's IgG Antibody Responses to
879 Routine Vaccines 2 Years Later and Anti-Schistosome and Anti-Malarial Responses by
880 Neonates in Western Kenya. *Front Immunol.* 2018;9:1402.

- 881 76. Mewamba EM, Nyangiri OA, Noyes HA, Egesa M, Matovu E, Simo G. The Genetics of
882 Human Schistosomiasis Infection Intensity and Liver Disease: A Review. *Front Immunol.*
883 2021;12:613468.
- 884 77. Lund AJ, Sokolow SH, Jones IJ, Wood CL, Ali S, Chamberlin A, et al. Exposure, hazard,
885 and vulnerability all contribute to *Schistosoma haematobium* re-infection in northern Senegal.
886 *PLoS Negl Trop Dis.* 2021;15(10):e0009806.
- 887 78. Nkurunungi G, Zirimenya L, Nassuuna J, Natukunda A, Kabuubi PN, Niwagaba E, et al.
888 Effect of intensive treatment for schistosomiasis on immune responses to vaccines among rural
889 Ugandan island adolescents: randomised controlled trial protocol A for the 'POPulation
890 differences in VACcine responses' (POPVAC) programme. *BMJ Open.* 2021;11(2):e040426.
- 891 79. Nkurunungi G, Zirimenya L, Natukunda A, Nassuuna J, Oduru G, Ninsiima C, et al.
892 Population differences in vaccine responses (POPVAC): scientific rationale and cross-cutting
893 analyses for three linked, randomised controlled trials assessing the role, reversibility and
894 mediators of immunomodulation by chronic infections in the tropics. *BMJ Open.*
895 2021;11(2):e040425.
- 896 80. Corstjens PL, Li S, Zuiderwijk M, Kardos K, Abrams WR, Niedbala RS, et al. Infrared
897 up-converting phosphors for bioassays. *IEE Proc Nanobiotechnol.* 2005;152(2):64-72.
- 898 81. Metcalf TU, Cubas RA, Ghneim K, Cartwright MJ, Grevenynghe JV, Richner JM, et al.
899 Global analyses revealed age-related alterations in innate immune responses after stimulation of
900 pathogen recognition receptors. *Aging Cell.* 2015;14(3):421-32.
- 901 82. Brown EP, Licht AF, Dugast AS, Choi I, Bailey-Kellogg C, Alter G, et al. High-
902 throughput, multiplexed IgG subclassing of antigen-specific antibodies from clinical samples. *J*
903 *Immunol Methods.* 2012;386(1-2):117-23.
- 904 83. Cinelli CaHC. Making sense of sensitivity: extending omitted
905 variable bias. *Journal of the Royal Statistical Society Series B (Statistical Methodology).*
906 2020;82(1):39-67.
- 907

908 **Figure captions**

909 **Fig 1. Clinical study design.** Participants enrolled in the clinical study (n =79, four donor samples were
910 unavailable for analysis in this study) were vaccinated at baseline [(pre-vaccination) day 0 (D0)] and
911 received two boosters at month 1 (M1) and month 6 (M6). Individuals provided sera samples at D0,
912 month 7 post-vaccination (M7) (one month post-booster 2) and month 12 post-vaccination (M12) (six
913 months post-booster 2), which were used to screen for Hepatitis B (HepB) antibody titers. Enrollees were
914 treated at day 12 post-vaccination (D12) with Praziquantel (PZQ) as appropriate, for egg counts detected
915 in stool samples which were collected at D0 (and day 3 and/or day 7). Sera samples at D0 were also used
916 to evaluate for schistosome-specific antigen (circulating anodic antigen, CAA). PMBCs and plasma were

917 also collected at D0, D12, M7 and M12 for subsequent analysis. X denotes corresponding samples
918 collected at that timepoint.

919

920 **Fig 2. Higher CAA concentration pre-vaccination is associated with a reduction in Hepatitis B**

921 **vaccine titers.** (A) Density of Schistosome-specific antigen values (CAA [pg/ml]) analyzed in serum

922 samples from participants pre-vaccination (D0). A binomial distribution was fitted to the CAA values and

923 a maximum-likelihood was used to identify the optimum cutoff separating the two modes of the CAA

924 values. Two groups of participants were then identified based on CAA values, low CAA (<36pg/mL

925 CAA), n =41; and high CAA (\geq 36pg/mL CAA), n =33. Male (blue line), n =53; Female (red line), n =21

926 (B) Hepatitis B (HepB) titers (log pg/mL) determined by commercial immunoassays for individuals at

927 M7 post-vaccination plotted to compare low and high CAA. Participants were further defined based on

928 CAA concentration values using methodology from the CAA assay that allowed detection of samples as

929 low as 3pg/mL: non-infected [no] (<3pg/mL CAA), low CAA [low] (3-100 pg/mL CAA), and high CAA

930 [high] (>100pg/mL CAA) (C) HepB titers for individuals at Month 7 post-vaccination, non-infected, n

931 =16, low CAA, n =26 and high CAA, n =22 and (D) Month 12 post-vaccination, non-infected, n =14, low

932 CAA, n =23, and high CAA, n =19 plotted to compare CAA. Boxplots show median values (horizontal

933 line), interquartile range (box) and 95% confidence interval (whiskers).

934

935 **Fig 3. Elevated levels of plasma cytokines/chemokines involved in lymphocyte cell migration and**

936 **activation pre-vaccination in individuals with *S. mansoni* infection persist at month 12 post-**

937 **vaccination.** (A) CCL17, (B) CCL19, and (C) CXCL9 levels in the plasma of non-infected individuals

938 pre-vaccination (D0), n =19, low CAA, n =32, and high CAA, n =24, and M12 post-vaccination, n =15,

939 low CAA, n =29, and high CAA, n =19. Data shown as \pm SEM. * $P \leq 0.05$. Wilcoxon rank-sum test

940 performed on non-infected vs. low CAA, or non-infected vs. high CAA, or low CAA vs. high CAA

941 within each time point D0 or M12. Non-infected- light grey, low CAA - blue, and high CAA - dark grey.

942 (D) Principal component analysis of plasma cytokines/chemokines pre-vaccination and after Hepatitis B

943 vaccination was conducted and the first (PC1) and second (PC2) principal components were used to plot
944 samples based on their plasma cytokines/chemokines profiles. Each dot corresponds to a sample and
945 colors denote the timepoint the sample was collected: D0- red, D3- green, D7- blue, and M12- purple.

946

947 **Fig 4. Frequencies of circulating follicular helper (cTfh) cells are lower pre- and post-vaccination in**

948 ***S. mansoni* infection with concurrent higher frequencies of regulatory T cells (Tregs) in individuals**

949 **with high CAA concentration.** Frequencies of CD3⁺CD4⁺CD45RA⁻CD25⁻CXCR5⁺, populations: (A)

950 cTfh1 [CXCR3⁺], (B) cTfh2 [CXCR3⁻CCR6⁻], (C) cTfh17 [CXCR3⁻CCR6⁺], (D) non cTfh

951 [CD3⁺CD4⁺CD45RA⁻CD25⁻CXCR5⁻] and (E) CXCR5⁻Tregs [CD3⁺CD4⁺CD45RA⁻CD127⁻

952 CD25⁺Foxp3⁺CXCR5⁻] were identified by flow cytometry of PBMCs from individuals pre-vaccination

953 (D0) non-infected, n =19, low CAA, n =31, and high CAA, n =25, M7 post-vaccination non-infected, n

954 =14, low CAA, n =17, and high CAA, n =20, and M12 post-vaccination non-infected, n =16, low CAA, n

955 =24, and high CAA, n =20. Data shown as ± SEM. *P ≤ 0.05. Wilcoxon rank-sum test performed on non-

956 infected vs. low CAA, or non-infected vs. high CAA, or low CAA vs. high CAA for each time point

957 separately D0, M7, or M12. Non-infected- light grey, low CAA - blue, and high CAA - dark grey.

958

959 **Fig 5. Frequencies of antibody secreting cells (ASCs) are lower at month 12 post-vaccination in**

960 **individuals with high CAA concentration.** Frequencies of (A) KI67⁺ ASCs [CD19⁺CD10⁻IgD⁻

961 CD71⁺CD38⁺CD20⁻], (B) IgG⁺ ASCs, and (C) IgA⁺ ASCs, were identified by flow cytometry of PBMCs

962 from individuals pre-vaccination (D0) non-infected, n =16, low CAA, n =29, and high CAA, n =24, M7

963 post-vaccination non-infected, n =14, low CAA, n =17, and high CAA, n =20, and M12 post-vaccination

964 non-infected, n =16, low CAA, n =23, and high CAA, n =21. Data shown as ± SEM. * P ≤ 0.05.

965 Wilcoxon rank-sum test performed on non-infected vs. low CAA, or non-infected vs. high CAA, or low

966 CAA vs. high CAA for each time point separately D0, M7, or M12. Non-infected- light grey, low CAA -

967 blue, and high CAA - dark grey.

968

969 **Fig 6. Changes in the Ig isotype profile are evident in *S. mansoni* infection pre- and post-vaccination**
970 **in response to TLR9 stimulation.** (A) IgG4 levels pre-vaccination (D0), and (C) IgA levels at M12 post-
971 vaccination in the culture supernatant of PBMCs stimulated for 7 days with CpG (CpG-ODN [TLR9]) or
972 UNT (untreated). D0 non-infected, n =14, low CAA, n =27, and high CAA, n =21, and M12 post-
973 vaccination non-infected, n =10, low CAA, n =20, and high CAA, n =17. Data shown as \pm SEM. * $P \leq$
974 0.05. Wilcoxon matched-pairs signed rank test performed on UNT vs. CpG for each non-infected, or low
975 CAA, or high CAA, and within the CpG-treated group a Wilcoxon rank-sum test on non-infected vs. low
976 CAA, or non-infected vs. high CAA, or low CAA vs. high CAA. Non-infected- light grey, low CAA -
977 blue, and high CAA - dark grey. (B) The mean Florescence intensity (MFI) of serum *S. mansoni*-specific
978 IgG4 at D0 non-infected [no], n =15, low CAA [low], n =21, and high CAA [high], n =20). A student t-
979 test was used to evaluate for the significance of the correlation. $P \leq 0.05$ was considered significant.

980
981 **Fig 7. Hepatitis B peptide-specific memory CD4⁺ T cells positively correlate with Hepatitis B titers**
982 **at month 7 post-vaccination, with a concurrent negative correlation for Hepatitis B peptide-specific**
983 **memory CD8⁺ T cells.** Frequencies of CFSE⁻ (A) CD4⁺CD45RA⁻ memory T (CD4⁺ mem), and (B)
984 CD8⁺CD45RA⁻ memory T cells (CD8⁺ mem), were identified by flow cytometry of PBMCs from
985 individuals at M7 post vaccination non-infected, n =12, low CAA, n =10, and high CAA, n =15, that were
986 stimulated for 6 days with hepatitis B long envelope protein peptide (HBV LEP) or DMSO control
987 (control). Data shown as \pm SEM. * $P \leq 0.05$. Wilcoxon matched-pairs signed rank test performed on
988 control vs. HBV LEP for each non-infected, or low CAA, or high CAA, and within the HBV-LEP-treated
989 group a Wilcoxon rank-sum test on non-infected vs. low CAA, or non-infected vs. high CAA, or low
990 CAA vs. high CAA within the CpG-treated. Non-infected- light grey, low CAA - blue, and high CAA -
991 dark grey. (C) Linear regressions were fit between Hepatitis B titers and CFSE⁻ (C) CD4⁺ mem, and (D)
992 CD8⁺ mem T cell populations adjusted for sex and student t-tests were used to evaluate for the
993 significance of the association. t (t-statistic). $P \leq 0.05$ was considered significant. (Shape: triangle-Male,
994 circle-Female; color: grey- non-infected, black- low CAA, blue- high CAA).

995

996 **Fig 8. Monocyte function is important in and significantly correlate with Hepatitis B vaccine**
997 **responses.** Antibody-dependent cellular phagocytosis (ADCP) assays with serum from individuals pre-
998 vaccination, non-infected, n =14, low CAA, n =20, and high CAA, n =18, were conducted with cells from
999 the monocyte cell line THP-1. Scatter plots show HBsAg-specific ADCP associations with (A) Hepatitis
1000 B titers at M12, and with (B) HBsAg-specific IgG1, and (C) HbsAg-specific antibody binding to
1001 FcγR3A (CD16) expression determined by antibody subclass and Fc receptor binding assays using serum
1002 samples from pre-vaccinated individuals. Spearman correlation and t-test were used to evaluate for the
1003 significance of the correlation. *coef* (regression coefficient). *t* (t-statistic). $P \leq 0.05$ was considered
1004 significant. (Shape: triangle-Male, circle-Female; color: grey- non-infected, black- low CAA, blue- high
1005 CAA).

1006

1007 **Fig 9. Lower levels of cytokines/chemokines important in the activation and maturation of innate**
1008 **immune cells in *S. mansoni*-infected individuals pre-vaccination and day 12 post-vaccination.** (A)
1009 CXCL10 levels pre-vaccination (D0) non-infected, n =19, low CAA, n =31, and high CAA, n =25, and
1010 (B) CCL19, (C) CCL26, (D) CCL27, (E) IL-1 β , and (F) IL-10 levels at D12 post vaccination non-
1011 infected, n =15, low CAA, n =26, and high CAA, n =23], in the culture supernatant of PBMCs stimulated
1012 for 18 hours with CLO97 (TLR7/8 agonist) or untreated (UNT). Data shown as \pm SEM. * $P \leq 0.05$
1013 Wilcoxon matched-pairs signed rank test performed on UNT vs. CLO97 or each non-infected, or low
1014 CAA, or high CAA, and within the CLO97-treated group a Wilcoxon rank-sum test on non-infected vs.
1015 low CAA, or non-infected vs. high CAA, or low CAA vs. high CAA. Non-infected- light grey, low CAA
1016 - blue, and high CAA - dark grey.

1017

1018 **Supporting information captions**

1019 **S1 Fig. Elevated plasma cytokines/chemokines in *S. mansoni*-infected individuals pre-vaccination.**
1020 (A) CCL7, (B) CCL11, (C) CCL22, (D) CCL24, (E) IL-2, and (F) M-CSF levels in the plasma of non-

1021 infected, n = 19, low CAA, n = 32, and high CAA, n = 24, individuals pre-vaccination (day 0). Data
1022 shown as \pm SEM. * $P \leq 0.05$. Wilcoxon rank-sum test performed on non-infected vs low CAA, or non-
1023 infected vs high CAA, or low CAA vs high CAA for each time point separately. Non-infected- light grey,
1024 low CAA - blue, and high CAA - dark grey.

1025

1026 **S2 Fig. CCL17 and soluble IL-2R levels in individuals with *S. mansoni* infection correlate with**

1027 **Hepatitis B titers post-vaccination.** Scatter plots of Hepatitis B titers at M12 as a function of (A-B)

1028 CCL17 and (D-E) soluble IL-2R cytokine levels in the plasma of non-infected participants at D0, n =19,

1029 low CAA, n =32, and high CAA, n =24, and M12 post-vaccination, n =15, low CAA, n =29, and high

1030 CAA, n =19. $P \leq 0.05$. Linear regressions were fit between Hepatitis B titers and the cytokines adjusted

1031 for sex and student t-tests were used to evaluate for the significance of the association. t (t-statistic). $P \leq$

1032 0.05 was considered significant. (Shape: circle-females, triangle-males; color: grey- non-infected, black-

1033 low CAA, blue- high CAA). (C) Soluble IL-2R levels in the plasma of non-infected individuals pre-

1034 vaccination (D0), n =19, low CAA, n =32, and high CAA, n =24, and M12 post-vaccination, n =15, low

1035 CAA, n =29, and high CAA, n =19. Non-infected- light grey, low CAA - blue, and high CAA - dark grey.

1036

1037 **S3 Fig. Flow cytometry gating strategy for T cell populations.** Representative plots showing non-

1038 circulating T follicular helper cells (cTfh) populations as $CD3^+CD4^+CD45RA^-CD25^-CXCR5^-$ and cTfh

1039 populations as $CD3^+CD4^+CD45RA^-CD25^-CXCR5^+$, identifying cTfh1 as $CXCR3^+$, cTfh2 as $CXCR3^-$

1040 $CCR6^-$, and cTfh17 as $CXCR3^-CCR6^+$. Regulatory T cells (Tregs) were identified as

1041 $CD3^+CD4^+CD45RA^-CD127^-CD25^+Foxp3^+$.

1042

1043 **S4 Fig. Flow cytometry gating strategy for B cell populations.** Representative plots showing activated

1044 B cells (ABC) as $CD19^+CD10^-IgD^-CD71^+CD38^-CD20^+$ and antibody secreting B cells (ASC) as

1045 $CD19^+CD10^-IgD^-CD71^+CD38^+CD20^-$.

1046

1047 **S5 Fig. Frequencies of Activated B cells (ABC) were elevated in *S. mansoni* infection pre- and post-**
1048 **vaccination.** Frequencies of (A) ABCs [CD19⁺CD10⁻IgD⁻CD71⁺CD38⁻CD20⁺], and (B) IgG⁺ ABCs,
1049 were identified by flow cytometry of PBMCs from individuals pre-vaccination (D0) non-infected, n = 16,
1050 low CAA, n = 29, and high CAA, n = 24], M7 post-vaccination non-infected, n = 14, low CAA, n = 17,
1051 and high CAA, n = 20, and M12 post-vaccination non-infected, n = 16, low CAA, n = 23, and high CAA,
1052 n = 21. Data shown as ± SEM. * P ≤ 0.05. Wilcoxon rank-sum test performed on non-infected vs low
1053 CAA, or non-infected vs high CAA, or low CAA vs high CAA for each time point separately D0, M7, or
1054 M12. Non-infected- light grey, low CAA - blue, and high CAA - dark grey. (C) Linear regressions were
1055 fit between Hepatitis B titers and IgA⁺ ASCs adjusted for sex and student t-tests were used to evaluate for
1056 the significance of the association. t (t-statistic). P ≤ 0.05 was considered significant. (Shape: triangle-
1057 Male, circle-Female; color: grey- non-infected, black- low CAA, blue- high CAA).

1058
1059 **S6 Fig. Plasma IgE is elevated pre-vaccination and remains elevated at month 12 post-vaccination**
1060 **in *S. mansoni*-infected individuals.** Plasma IgE levels pre-vaccination (D0) and M12 post-vaccination.
1061 D0 non-infected, n = 17, low CAA, n = 20, and high CAA, n = 19], and M12 post-vaccination non-
1062 infected, n = 15, low CAA, n = 26, and high CAA, n = 20. Data shown as ± SEM. * P ≤ 0.05. Wilcoxon
1063 rank-sum test performed on non-infected vs low CAA, or non-infected vs high CAA, or low CAA vs high
1064 CAA for each time point separately D0, or M12. Non-infected- light grey, low CAA - blue, and high
1065 CAA - dark grey.

1066
1067 **S7 Fig. Flow cytometry gating strategy for monocyte populations.** Representative plots showing non-
1068 classical (NC) monocytes as CD3⁻CD19⁻CD14^{dim}CD16⁺, classical monocytes (CL) as CD3⁻CD19⁻
1069 CD14⁺CD16⁺, and intermediate monocytes (INT) as CD3⁻CD19⁻CD14⁺CD16⁻.

1070
1071 **S8 Fig. Flow cytometry gating strategy for monocyte populations.** Frequencies of monocyte
1072 populations (A) (classical [CD3⁻CD19⁻CD14⁺CD16⁺], (B) intermediate [CD3⁻CD19⁻CD14⁺CD16⁻], and

1073 (C) non-classical [CD3⁻CD19⁻CD14^{dim}CD16⁺] were identified by flow cytometry of PBMCs from
1074 individuals pre-vaccination, non-infected, n =14, low CAA, n =20, and high CAA, n =18. Non-infected-
1075 light grey, low CAA - blue, and high CAA - dark grey. (D-F) Scatter plot showing the frequencies of
1076 monocytes subsets as a function of Hepatitis B titers at M7 post-vaccination. Linear regressions were fit
1077 between Hepatitis B titers and the monocyte subset frequencies adjusted for sex and experiment batch,
1078 and student t-tests were used to evaluate for the significance of the association. Spearman correlation and
1079 t-test were used to evaluate for the significance of the correlation. *coef* (regression coefficient), *t* (t-
1080 statistic). $P \leq 0.05$ was considered significant.

1081

1082 **S1 Table.** Study participant information.

1083

1084 **S2 Table.** Statistical information for plasma Luminex cytokine/chemokine levels.

1085

1086 **S3 Table.** Sensitivity analysis for plasma Luminex cytokine/chemokine levels correlated with Hepatitis B
1087 titers.

1088

1089 **S4 Table.** Statistical information for Frequency of T cells.

1090

1091 **S5 Table.** Statistical information for Frequency of B cells.

1092

1093 **S6 Table.** Sensitivity analysis for B cell flow cytometry frequencies correlated with Hepatitis B titers.

1094

1095 **S7 Table.** Statistical information for supernatant cytokine/chemokine levels from CLO97-stimulated
1096 PBMCs.

1097


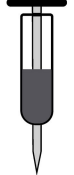
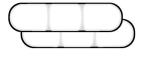
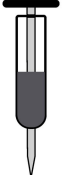
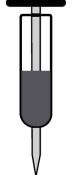
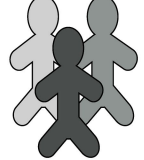
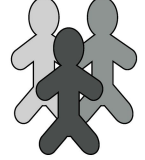
1098 **S8 Table.** Ex vivo T cell staining panel for PBMCs.

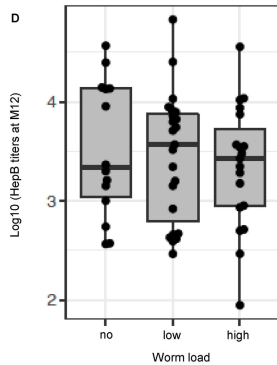
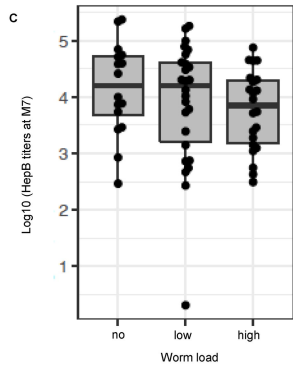
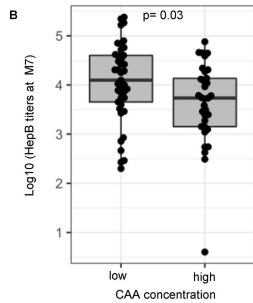
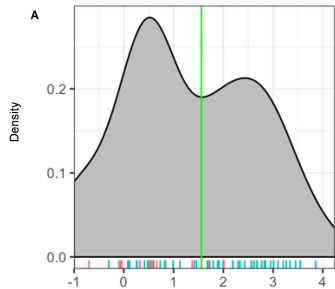
1099

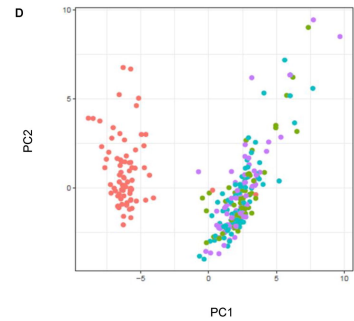
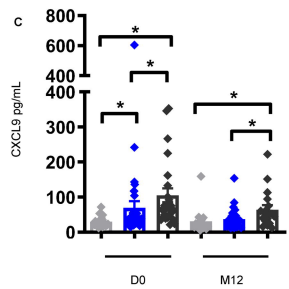
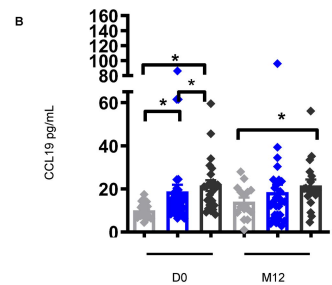
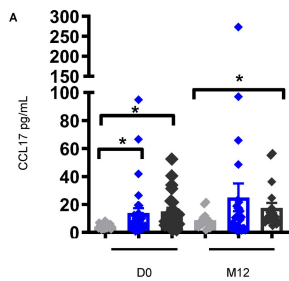
1100 **S9 Table.** Ex vivo B cell staining panel for PBMCs.

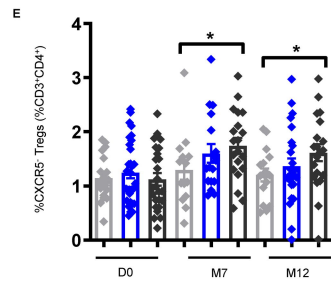
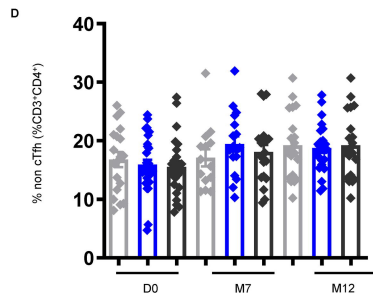
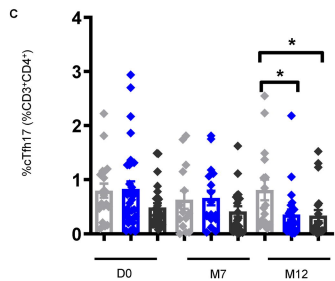
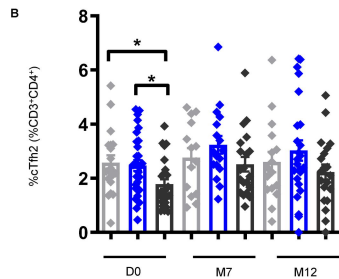
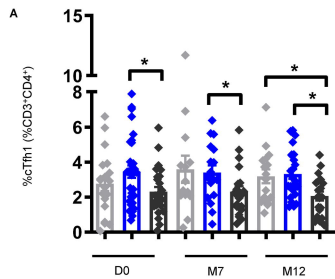
1101

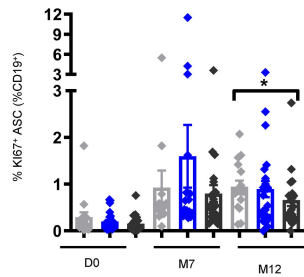
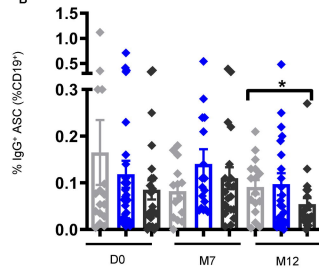
1102 **S10 Table.** T cell staining panel for PBMCs after Hepatitis B peptide stimulation.

| Day (D) Month (M) | D0 | D12 | M1 | M6 | M7 | M12 | |
|----------------------------|--|---|--|--|--|---|---|
| |  Pre-vaccine Baseline <i>n</i> =79 |  Hep B Vaccine |  Worm Treatment |  Hep B Vaccine Boost |  Hep B Vaccine Boost |  1 month post 2nd Boost <i>n</i> =64 |  6 months post 2nd Boost <i>n</i> =64 |
| HepB Ab Titers | X | | | | X | X | |
| CAA | X | | | | | | |
| Harvest PBMCs Plasma | X | X | | | X | X | |







A**B****C**